Thallium Oscillator Strengths and $6d\ ^2D_{3/2}$ State hfs*

ALAN GALLAGHER AND ALLEN LURIO
IBM Watson Laboratory, Columbia University, New York, New York
(Received 14 May 1964)

The lifetime of the $7\ ^2S_{1/2}$ state of thallium has been measured by the optical-double-resonance technique, with the result $\tau=7.4\pm0.3\times10^{-9}$ sec, and by the level-crossing technique, with the result $\tau=7.6\pm0.2\times10^{-9}$ sec. The intensity ratio of the $7\ ^2S_{1/2}$-$6\ ^2P_{3/2}$ and $7\ ^2S_{1/2}$-$6\ ^2P_{1/2}$ lines radiated by an optically pumped thallium beam was measured to establish the oscillator-strength ratio for these two transitions. The result is $A_{5350}/A_{3776}=1.16\pm0.05$. The lifetime and hfs of the thallium $6\ ^2D_{3/2}$ state were measured by the level-crossing technique. The results are $\tau=6.2\pm1\times10^{-9}$ sec and $|a|/h=41\pm2\times10^6$/sec. (The Tl^{205} and Tl^{203} hfs were not resolved in the experiment.) A table of thallium oscillator strengths has been constructed from our results and from some of the oscillator-strength ratios reported in the literature. The values in the table are compared to those in the remainder of the literature in order to collect and comment on equivalent values from other experiments. The oscillator-strength values in the table are also compared to the predictions of Bates and Damgaard's and Vainshtein's approximation methods. It was found that when $n_p^*<2$, the $s-p$ transition probabilities calculated by extrapolating the tables of Bates and Damgaard are quite different from the values directly calculated using their theory. The directly calculated Bates-Damgaard values are in much better agreement with the experimental results (the average difference is 17% for 20 thallium transition). Vainshtein's calculated $7\ ^2S_{1/2}$ to $6\ ^2P_{1/2,3/2}$ oscillator strengths differ from our experimental values by an average of 15%. The measured $6\ ^2D_{3/2}$ state hfs is in excellent agreement with the prediction of the Fermi-Segrè formula if a is assumed positive. Nonetheless, configurational mixing is expected to influence this hfs, and the effect of $ss'd$ and sp^2 configurational mixing has been calculated in terms of unknown mixing coefficients. From estimates of the magnitudes of these coefficients, it would appear that the above agreement is coincidental, and the Tl D state hfs should be quite sensitive to the amount of mixing.

I. INTRODUCTION

THE oscillator strengths of the spectral lines of Tl I have been the subject of many experimental investigations, principally because they involve the transitions of a single unpaired electron and because of the relative ease with which thallium resonance radiation can be produced. The major portion of the experimental data on Tl oscillator strengths is the result of the measurements of anomalous dispersion (AD) by a Tl vapor in the neighborhood of a spectral line.[1] The AD method developed by Rozhdestvenski has been employed by several Russian groups to accurately establish the ratios of the oscillator strengths of many transitions to the Tl $6p$ levels. The absolute values of oscillator strengths can also be determined in AD experiments if the density of the vapor is known, but the wide range of conflicting absolute values quoted in various AD experiments is testimony to the difficulties involved in determining the actual density of the vapor. This difficulty has now been partially overcome by taking an improved thermodynamic approach to determine the vapor density,[2] but uncertainies of about 20% are apparently still present. Thus, the ratios of many of the Tl oscillator strengths have been accurately measured, but the absolute values of these oscillator strengths are still somewhat uncertain due to the large number of conflicting experimental results. Accurate values for a few appropriate oscillator strengths can thus be used to accurately establish many additional values.

In order to improve the accuracy with which the absolute oscillator strengths of the Tl I spectrum are known, we have measured the lifetime of the $7s\ ^2S_{1/2}$ state by two independent experimental methods; namely, by the zero-field level-crossing method and by the optical-double-resonance method. Our observation of the zero-field level crossing in the $^2S_{1/2}$ state demonstrates a new level-crossing technique for measuring lifetimes in $J=\frac{1}{2}$ atomic states. Since $1/\tau(7\ ^2S_{1/2})=A(7\ ^2S_{1/2}\text{-}6\ ^2P_{1/2})+A(7\ ^2S_{1/2}\text{-}6\ ^2P_{3/2})$, a measurement of the ratio $A(7\ ^2S_{1/2}\text{-}6\ ^2P_{3/2})/A(7\ ^2S_{1/2}\text{-}6\ ^2P_{1/2})$ will establish these two A values from the $7\ ^2S_{1/2}$ state lifetime. [$\tau(a)$ = lifetime of state a, $A(a\text{-}b)$ = transition probability per sec of the a-b transition, $A(a\text{-}b)$ is proportional to the oscillator strength $f(a\text{-}b)$.] This ratio has been measured three times, but the result that should be the most accurate[3] disagrees with the results of the other two experiments by more than 10%.[4,5] Consequently, we have made an independent measurement of this ratio by measuring the relative intensities of the $7\ ^2S_{1/2}$-$6\ ^2P_{1/2}$ and $7\ ^2S_{1/2}$-$6\ ^2P_{3/2}$ fluorescence lines from an atomic beam of Tl excited by $7\ ^2S_{1/2}$-$6\ ^2P_{1/2}$ resonance radiation. We have thus been able to establish the $A(7\ ^2S_{1/2}\text{-}6\ ^2P_{1/2})$ and $A(7\ ^2S_{1/2}\text{-}6\ ^2P_{3/2})$ from our measurements. The relative oscillator-strength results of several AD experiments have then been used to calculate, from these two A values, the absolute values of many oscillator strengths of the five series of transitions

* This article is based on a thesis presented to Columbia University by Alan Gallagher in partial fulfillment of the requirements for the Ph.D. degree, February, 1964.

[1] C. G. Mitchel and M. W. Zemansky, *Resonance Radiation and Excited Atoms* (Cambridge University Press, 1961), 2nd ed.

[2] I. Gurvich, Opt. i Spektroskopiya **5**, 205 (1958).

[3] G. Kvater, Zh. Eksperim. i Teor. Fiz. **11**, 421 (1941).

[4] O. Vonweiler, Phys. Rev. **35**, 802 (1930).

[5] V. Prokofiev and V. Soloviev, Z. Physik **48**, 276 (1958).

to the $6\,^2P_J$ levels. We have also measured the lifetime of the $6d\,^2D_{3/2}$ state by the level-crossing technique, thus providing a check on $1/\tau(6\,^2D_{3/2}) = A(6\,^2D_{3/2}\text{-}6\,^2P_{1/2}) + A(6\,^2D_{3/2}\text{-}6\,^2P_{3/2})$.

If configurational mixing is neglected, the Tl I states are (core) $6s^2nl$ configurations and the atomic oscillator strengths correspond to the oscillator strengths of the single valence electron. The only approximation techniques which have been extended to calculating Tl oscillator strengths are those of Bates and Damgaard without configurational mixing and Vainshtein without configurational mixing but including interaction with the core. Bates and Damgaard[6] (B & D) have utilized the fact that the oscillator strengths depend primarily on the transition-electron wave functions outside the core to develop their "Coulomb approximation" method. This theory has been quite successful in predicting many oscillator strengths of heavy and light elements, although it has seemed to be considerably in error for thallium. L. Vainshtein[7] has developed analytical approximation methods which treat in more detail the effect of the core on the external-electron radial functions, and he has been able to improve on the B & D oscillator-strength results for many elements. He has, so far, published results for only $A(7\,^2S_{1/2}\text{-}6\,^2P_{3/2})$ of thallium,[8] but he has also communicated to Ostrovskii and Penkin[9] an earlier result for $A(7\,^2S_{1/2}\text{-}6\,^2P_{1/2})$ and his method appears to be capable of calculating additional values.

The ratio of the hfs separation to linewidth of the $6\,^2D_{3/2}$ state of thallium limited the accuracy of this $|a|$ determination to $\pm 5\%$, while the dipole moments of the natural thallium isotopes (70% Tl^{205}, 30% Tl^{203}) differ by only 1%. Consequently, the Tl^{205} and Tl^{203} hfs were not resolved, and $|a|$ is an average of the two isotopic values. The $6d\,^2D_{3/2}$ state hfs, as well as many of the Tl oscillator strengths, may be expected to reflect the influence of configuration interaction. The effects of configuration interaction on hfs were first analyzed by Fermi and Segrè, who considered Tl I and the structurally equivalent Pb II as examples.[10] In 1952, Koster[11] found reasonable agreement between the measured hfs of the $4\,^2P_{1/2,3/2}$ levels of gallium and the values he calculated using Hartree functions and mixing of the $4s5s5p$ configuration into the $4s^24p$ configuration. Schwartz,[12] in his theory of hfs, calculated the effect of the mixing on the hfs anomaly in the $4\,^2P_{1/2,3/2}$ levels of Ga. He later calculated the hfs anomaly in the $6\,^2P_{1/2,3/2}$ states of Tl^{203} and Tl^{205} using $6sns6p$ configuration mixing, and the theoretical ratio of $^2P_{1/2}$ and $^2P_{3/2}$ state anomalies is in good agreement with the experimental value.[13] The ratio of the hfs to the linewidth is not large enough to allow a measurement of the hfs anomaly in the $n\,^2D_{3/2,5/2}$ states of thallium, but the hyperfine interactions of $6s^2nd$ configurations are so small that very slight mixing with configurations having unpaired s electrons can be important. The oscillator strengths will not be as sensitive to the mixing, but variations even larger than the experimental versus theoretical differences in Table I appear quite likely.

Unfortunately, no wave functions with which the mixing coefficients can be checked are yet available for thallium, so that these effects can only be calculated in terms of unknown mixing coefficients. We have calculated the expected $n\,^2D_{3/2}$ hfs in terms of unknown mixing coefficients of the $6s6snd$ and $6s6p^2$ configurations and the magnitudes of these mixing coefficients have been inferred from other hfs of Tl I and Pb II, but the results must remain inconclusive until the appropriate wave functions are computed.

The paper has been arranged into separate descriptions of the four experiments, followed by a description of the resonance lamps used. Then, under the heading "Thallium Oscillator Strengths," the table of oscillator strengths is generated and comparisons are made with the results of other experiments and with the predictions of the two theories. Finally, the measured $6\,^2D_{3/2}$ state hfs is compared to the theoretical predictions of this hfs.

II. OPTICAL DOUBLE-RESONANCE MEASUREMENT OF THE $7s^2S_{1/2}$ STATE LIFETIME

In this experiment $\tau(7\,^2S_{1/2})$ was determined from the linewidth of the optically detected, magnetic-resonance signal between the $F=1$ Zeeman levels of the $7\,^2S_{1/2}$ state. (The pertinent hyperfine levels are shown in Fig. 1.) In this application of the double-resonance technique we used the following experimental arrangement (see Fig. 2). Circularly polarized 3776 Å resonance radiation traveling parallel to an externally applied, static magnetic field H_0 was incident on a quartz cell containing thallium vapor. This radiation excited thallium atoms from the (ground) $6\,^2P_{1/2}$ state to the $7\,^2S_{1/2}$ state, from which state about half decayed to the $6\,^2P_{3/2}$ state emitting 5350 Å radiation and the other half decayed back to the ground state. A phototube and analyser detected the intensity of one circularly polarized component of the 5350 Å radiation propagating in the static-field direction. A rf magnetic field, of oscillating amplitude $2H_1$ and frequency ω, was applied to the vapor in a direction perpendicular to the static magnetic field. The 5350 Å decay radiation was detected since it can be optically filtered from the pumping radiation. This is particularly valuable in an experiment

[6] D. Bates and A. Damgaard, Trans. Roy. Soc. (London) **A242**, 101 (1949).
[7] L. Vainshtein, *Transactions of the P. N. Lededev. Physics Institute*, Vol. 15 (Translated by Consultants Bureau, New York, 1962).
[8] L. Vainshtein **22**, 671 (1958); Izv. Akad. Nauk SSSR Ser. Fiz. **22**, 671 (1958).
[9] Y. Ostrovskii and N. Penkin, Opt. i Spektroskopiya **4**, 719 (1958).
[10] E. Fermi and E. Segrè, Z. Physik **82**, 729 (1933).
[11] G. Koster, Phys. Rev. **66**, 148 (1952).
[12] C. Schwartz, Phys. Rev. **97**, 380 (1955), Eqs. (24), (26b), (31), (32), (46) and Discussion.
[13] G. Gould, Phys. Rev. **101**, 1828 (1956).

of this type where the optimum conditions are with the scattered radiation parallel to the incident radiation.

The 3776 Å exciting radiation produces $\Delta m=+1$ transitions from the $^2P_{1/2}$ to the $^2S_{1/2}$ state. The rate of excitation $R_{F,m}$ to the various $^2S_{1/2}$ sublevels is

$$R_{F,m}=\begin{vmatrix} R_{0,0} \\ R_{1,1} \\ R_{1,0} \\ R_{1,-1} \end{vmatrix} = G \begin{vmatrix} I_{10} \\ I_{01}+I_{11} \\ I_{11} \\ 0 \end{vmatrix}, \quad (1)$$

where I_{10}, I_{11}, and I_{01} are the effective intensities of the resolved hyperfine lines of the 3776 Å radiation, as defined in Fig. 1, and the proportionality constant, G, depends on the experimental geometry and on the Tl vapor pressure. By detecting $\Delta m=+1$ circularly polarized 5350 Å radiation propagating in the dc field direction, the following proportions $K_{F,m}$ of the spontaneous decay from the $^2S_{1/2}$ F, m sublevels are detected:

$$K_{F,m}=\begin{vmatrix} K_{0,0} \\ K_{1,1} \\ K_{1,0} \\ K_{1,-1} \end{vmatrix} = K_0 \begin{vmatrix} 2 \\ 3 \\ 2 \\ 1 \end{vmatrix}. \quad (2)$$

The common factor K_0 depends on the solid angle and optical losses in the detection system.

The intensity of the detected radiation is determined as a function of H_0 and H_1 by the following application of the theory of Bitter and Brossel.[14] From Eq. (1), $R_{F',m'}dt'$ is the number of ground-state atoms optically excited into the F', m' state during the time interval from t' to $t'+dt'$. At a time, $t>t'$, the number of these atoms still in the $^2S_{1/2}$ state is $R_{F',m'}dt' \exp[-(t-t')/\tau]$. The number of these atoms in each F, m sublevel at time t will be

$$n_{F,m;F',m'}(t,t)dt' = R_{F',m'}dt' P(F',m';F,m,t-t')e^{(-t+t')/\tau}, \quad (3)$$

where τ is the natural lifetime of the $^2S_{1/2}$ state, and $P(F',m';F,m,t-t')$ is the probability that an atom in the F', m' state at time t' is in the F, m state at time t if the finite lifetime, τ, is neglected. If one excites at a constant rate, $R_{F',m'}$ to each of the F',m' states from $t'=-\infty$ to t, then the total number of atoms in each F, m state at time t will be

$$\sum_{F'm'}\int_{-\infty}^{t} n_{F,m;F'm'}(t,t')dt' = \sum_{F'm'} R_{F',m'}\int_{-\infty}^{t} P(F',m';F,m,t-t')e^{(-t+t')/\tau}dt' = \sum_{F'm'} R_{F,'m'}P(F'm';F,m), \quad (4)$$

where

$$P(F',m';F,m)=\int_0^{\infty} e^{-t''/\tau}P(F',m';F,m,t'')dt''.$$

[14] J. Brossel and F. Bitter, Phys. Rev. 86, 308 (1952).

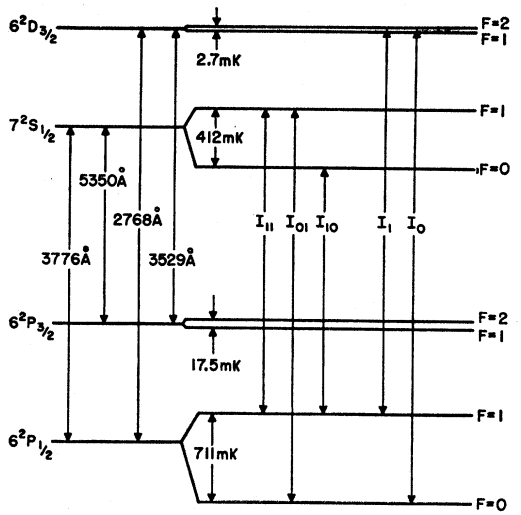

FIG. 1. Hyperfine structure intervals of four states of Tl^{205}. (The Tl^{203} intervals are about 1% smaller.) a is arbitrarily shown positive for the $6\,^2D_{3/2}$ state.

The spontaneous decay rate from each F, m level is $N_{F,m}/\tau$ and the proportion $K_{F,m}$ of the associated radiation is detected by the phototube. Thus, the phototube signal S is

$$S \propto \frac{1}{\tau}\sum_{F,m} K_{F,m}N_{F,m} = \frac{1}{\tau}\sum_{\substack{F,m \\ F',m'}} R_{F',m'}P(F'm';F,m)K_{F,m}. \quad (5)$$

In order to measure the linewidth of the transitions between the $F=1$ Zeeman levels, the rf oscillator was operated at a fixed frequency near 125 Mc/sec and the static magnetic field at the cell was swept from about 60 to 120 G through the resonance line. These conditions permit several simplifications to be made in evaluating Eq. (5). Since the hyperfine structure of the $7\,^2S_{1/2}$ state is 1.2×10^4 Mc/sec, the 125-Mc/sec rf field cannot cause any transitions between the $F=0$ and $F=1$ levels, and hence $P(0,0;1,m')=0$ and $P(0,0;0,0)=1$.

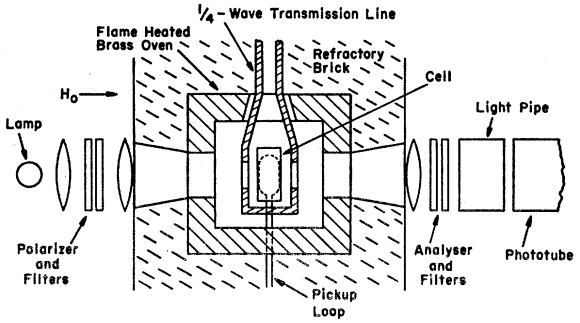

FIG. 2. Arrangement of the double-resonance experiment.

For the magnetic fields used in the experiment, the energy separations of the $^2S_{1/2}$, $F=1$ Zeeman levels are (from the Breit-Rabi equation) approximately

$$E_{1,1}-E_{1,0}\cong\hbar\gamma H_0\left(1-\frac{\hbar\gamma H_0}{a}\right),$$

$$E_{1,0}-E_{1,-1}\cong\hbar\gamma H_0\left(1+\frac{\hbar\gamma H_0}{a}\right),$$

$$\gamma=g_F(7\,^2S_{1/2},\,F=1)\frac{e}{2mc}=\frac{e}{2mc},\quad a=7\,^2S_{1/2}\text{ state hfs.}$$

In the experiment $\hbar\gamma H_0/a\cong 0.02$, and the approximate corrections, $\pm 0.02\hbar\gamma H_0$, to the linear-Zeeman-effect intervals are $\pm 6\%$ of the signal linewidth. Due to the complexity of the exact expression, we will calculate the signal shape with the approximation of equal energy separations, then estimate the corrections to this signal due to the unequal energy separations. We thus approximate the $P(1,m;1,m',t)$ in Eq. (4) by the three-level Majorana formula, which is strictly valid only in the linear Zeeman region.[15] [$P(1,m;1,m',t)$ is equivalent to $P(1,m,m',t)$ in the usual Majorana formula notation.] We then have [with $P(1,m;1,m')=P(1,m';1,m)$]

$$\begin{aligned}&P(1,1;1,0)=P(1,0;1,-1)=2\tau(A-C),\\ &P(1,1;1,-1)=\tau C,\\ &P(1,1;1,1)=P(1,-1;1,-1)=\tau(1-2A+C),\\ &P(1,0;1,0)=\tau(1-4A+4C).\end{aligned}\tag{6}$$

From Eqs. (1), (2), (5), and (6) we obtain for the phototube signal

$$S\propto 2I_{10}+2I_{11}+(3-2A)(I_{11}+I_{01}),\tag{7}$$

where

$$A\equiv A(\omega_0)=\frac{\frac{1}{2}(\gamma H_1)^2}{(\gamma H_1)^2+(1/\tau)^2+(\omega-\omega_0)^2},$$

$$C\equiv C(\omega_0)=\frac{3(\gamma H_1)^2A(\omega_0)}{4(\gamma H_1)^2+(1/\tau)^2+4(\omega-\omega_0)^2},\quad \omega_0=\gamma H_0.$$

To measure the resonance line shape, the rf magnetic-field amplitude was 100% square-wave modulated at 210 cps and the dc field swept through resonance. The output of the phototube was put through a lock-in detector synchronized to the rf modulation frequency, so that a signal proportional to the intensity difference at the phototube with the rf on and off was detected. Since A is zero when the rf is off, the detected signal is proportional to $(I_{11}+I_{01})A$. Thus,

$$S_{\text{Lock In}}\propto\frac{(\gamma H_1)^2}{(\gamma H_1)^2+(1/\tau)^2+(\omega-\gamma H_0)^2}.\tag{8}$$

[15] G. W. Series, Rept. Progr. Phys. 22, 280 (1959).

From Eq. (8) it can be seen that, with fixed H_1 and ω, a sweep of H_0 through resonance results in a Lorentzian-shaped signal of full half-amplitude width:

$$\Delta H_{1/2}=2[H_1^2+(1/\gamma\tau)^2]^{1/2},\tag{9}$$

which becomes $2/\gamma\tau$ as $H_1\to 0$.

We will now estimate the corrections to this signal shape due the nonlinear Zeeman effect. $P(1,m;1,m'\neq m)$, as defined in Eq. (4), is essentially the average probability of an rf-induced 1, m to 1, m' transition during the lifetime of the state. From Eqs. (6) and (7), it can be seen that when $(\gamma H_1\tau)^2\ll 1$, $P(1,m;1,m\pm 1)\leq(\gamma H_1\tau)^2\ll 1$, and the steady-state populations of the 1, m levels are not significantly altered by the rf. Thus when $(\gamma H_1\tau)^2\ll 1$, we can approximate the three-level system with two independent two-level systems (i.e., the 1, 1 and 1, 0, and the 1, 0 and 1, -1 systems). If the transitions probability for a two-level system, $P(\frac{1}{2},m,m\pm 1,t)$, is used in Eq. (4), the result is $P(\frac{1}{2},m,m\pm 1)=\tau A(\omega_0=\Delta E/\hbar)$, where ΔE is the energy separation of the pair of levels. Thus, for $(\gamma H_1\tau)^2\ll 1$, the $P(1,m;1m',t)$ in Eq. (6) can be corrected by dropping the C terms [which are $\propto(\gamma H_1\tau)^4$] and equating the correct energy separation to $\hbar\omega_0$ in the $A(\omega_0)$ associated with each pair of levels. [$P(\frac{1}{2},m,m\pm 1)/P(1,m,m\pm 1)\to 2$ as $\gamma H_1 t\to 0$ due to the F dependence of $\langle F,m|J\pm|F,m\pm 1\rangle$, but this should not confuse the identification of the ω_0 with $\Delta E/\hbar$.] In the experiment $(\gamma H_1\tau)^2=0.16$ at the maximum H_1 attained, so that these approximations should be sufficiently accurate for the evaluation of the corrections to the signal shape. We thus alter Eq. (6) to approximate the unequal spacing situation by taking [with $P(1,m;1,m')=P(1,m';1,m)$]

$$\begin{aligned}&P(1,1;1,0)\cong 2\tau A',\\ &P(1,1;1,1)\cong\tau(1-2A'),\\ &P(1,-1;1,0)\cong 2\tau A'',\\ &P(1,-1;1,-1)\cong\tau(1-2A''),\\ &P(1,1;1,-1)\cong 0,\\ &P(1,0;1,0)\cong\tau(1-2A'-2A'').\end{aligned}\tag{10}$$

where

$$A'=A[\omega_0=(E_{1,1}-E_{1,0})/\hbar],$$

$$A''=A[\omega_0=(E_{1,0}-E_{1,-1})/\hbar].$$

The lock-in signal, with these modifications, is proportional to $I_{11}A''+I_{01}A'$. For an unreversed lamp $I_{11}=2I_{01}$, and the ratio may vary to $I_{11}\ll I_{01}$ for a badly self-reversed lamp. In the latter case the signal has a peak at $\gamma H=\omega+0.06/\tau$ and a full half-amplitude width of $(1.02\times 2)/\gamma\tau$ (for $H_1\to 0$). In the intermediate case of $I_{11}=I_{01}$, the signal peak is at $\gamma H=\omega$ and the width is $2/\gamma\tau$ (for $H_1\to 0$); while in the $I_{11}=2I_{01}$ case the peak is at $\gamma H=\omega-0.02/\tau$ and the width is $(0.997\times 2)/\gamma\tau$ (for $H_1\to 0$). Since γH_{peak} was found to be always within $0.02/\tau$ of ω, it would appear from these argu-

ments that, for our lamp, an error of less than 1% is made by using Eq. (8) to determine τ from the signal shape. Since Eq. (10) is only an approximation, however, we will allow a 2% to 3% uncertainty due to the possibility of a systematic error from the use of Eq. (8).

To determine τ from the signal widths, a pickup loop was placed near the cell to detect a signal, V, proportional to H_1. The values of $(\Delta H_{1/2})^2$ measured over a range of H_1 values can then be plotted against V^2, and the extrapolation of a straight line through the data to $V=0$ intersects the axis, according to Eq. (9), at $\Delta H_{1/2}=2/\gamma\tau$. The linewidth data measured at vapor pressures between 10^{-4} to 10^{-7} mm over a period of a month and with two different cells is plotted in this manner in Fig. 3. Our conclusion $\tau=7.4\pm0.3\times10^{-9}$ sec is indicated on the same graph. The two circled points were not included in the determination of the lifetime, but are included on the plot to show the effects of "multiple-scattering narrowing" which appeared at high vapor pressures ($>10^{-4}$ mm) and at large values of $\gamma H_1\tau$. That the narrowing is only a few percent even at such large vapor pressures is not surprising, since the experimental conditions are not very different from those for which Barrat[16] calculates no narrowing for $^2S_{1/2}$ states.

The amount of broadening on the graph may be used to compute the amplitude of H_1 from Eq. (9). The result is that the maximum rf magnetic field used was $H_1=6.5$ G, which value agrees roughly with a calibration using a pickup loop in the cell position. Since the signal amplitude is proportional to H_1^2 for $\gamma H_1\tau\ll1$, these large fields were necessary for an accurate determination of τ. To obtain these large rf fields without causing gaseous breakdown in the cell, the 20-mm diameter, 10-mm deep, cylindrical cell was placed inside the shorted end of a $\frac{1}{4}$-wave transmission line which was driven by push-pull, 300-W Eimac tetrodes. The quartz cells were filled by thallium distillation from a bakeable vacuum system. Before distillation, the cells were baked at 900°C and then placed in a rf electric field to clean the walls by ion bombardment.

III. MEASUREMENT OF THE $7s^2S_{1/2}$ LIFETIME BY LEVEL CROSSING

In this experiment the width of the zero-field level crossing of the $7\,^2S_{1/2}$ state, $F=1$ Zeeman levels was measured to determine the lifetime of the $7\,^2S_{1/2}$ state. (The hyperfine levels are shown in Fig. 1.) 3776 Å radiation from a resonance lamp excited thallium atoms from the $6\,^2P_{1/2}$ (ground) state to the $7\,^2S_{1/2}$ state, and either 3776 or 5350 Å decay radiation was detected.

Breit[17] has calculated the average intensity of resonance fluorescence $\bar{S}$ from a gas of identical atoms excited by short pulses of optical radiation, and his result has now been verified in many level-crossing experiments. Franken[18] has shown how a more general white-light radiation field can also lead to Breit's fluorescence formula. This formula is

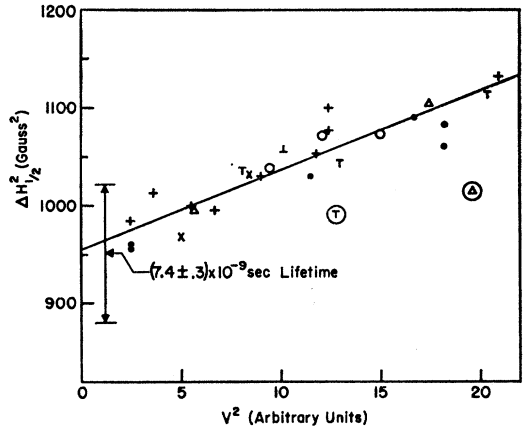

FIG. 3. Measured Lorentzian linewidths from the double-resonance experiment.

$$\bar{S}\propto\sum_{\substack{mm'\\ \mu\mu'}}\frac{f_{\mu m}f_{m\mu'}g_{\mu' m'}g_{m'\mu}}{\frac{1}{2}\tau_\mu+\frac{1}{2}\tau_{\mu'}+i\omega_{\mu\mu'}}, \tag{11}$$

where

$$f_{\mu m}=\langle\mu|\,\hat{e}\cdot\bar{P}\,|m\rangle,\quad g_{\mu m}=\langle\mu|\,\hat{e}'\cdot\bar{P}\,|m\rangle,$$
$$\omega_{\mu\mu'}=(E_\mu-E_{\mu'})/\hbar;$$

m and m' represent the quantum numbers of the ground-state sublevels and μ and μ' represent the excited states. $\hat{e}$ and $\hat{e}'$ are unit polarization vectors of the incident and scattered light, respectively. τ_μ is the lifetime of the μ state. The only external fields acting on the scattering atoms are a static magnetic field H and the optical radiation field $\bar{E}(t)$ representing the incident radiation from a lamp. An additional assumption is that the density of the vapor is sufficiently small so that no photon is scattered more than once. If the resonance radiation from the lamp is optically filtered, one can excite the scattering atoms only to the group of states which correspond to one value of n, l, J. The sum over μ and μ' need then be taken only over the quantum numbers F, m of the sublevels of this n, l, J state, and the lifetimes of all the excited states will be the same. Equation (11) applies to the case of uniform lamp power density throughout the frequency region necessary to produce all the $m\rightarrow\mu$ excitations. In our experiments, the exciting resonance radiation has resolved hyperfine lines of unequal amplitude so that Eq. (11) must be modified to fit this case. This has been done in Appendix I, and we will interpret this experiment by using the result [Eq. (25)].

It is necessary to excite with and detect circularly (or elliptically) polarized light to observe the Hanle effect

[16] J. Barrat, J. Phys. Radium **20**, 633 (1959).
[17] G. Breit, Rev. Mod. Phys. **5**, 91 (1933).
[18] P. Franken, Phys. Rev. **121**, 508 (1958).

in a $J=\frac{1}{2}$ state.[19] For circularly polarized light, the scattered intensity may be calculated from Eq. (24) by taking

$$\hat{e}=\frac{\hat{\theta}+\{\pm\}\hat{\varphi}}{\sqrt{2}} \quad \text{and} \quad \hat{e}'=\frac{\hat{\theta}'+\{\pm\}'\hat{\varphi}'}{\sqrt{2}}. \tag{12}$$

$\{\pm\}$ and $\{\pm\}'$ refer to left- or right-hand circular polarization, and the vectors $\hat{\theta}$ and $\hat{\varphi}$ are the spherical-coordinate unit vectors with the lamp radiation incident in the $-\hat{r}$ direction and the static magnetic field along the z axis. The primed vectors are also the spherical-coordinate unit vectors, but referred to the scattered radiation direction $\hat{r}'$. When detecting the 3776 Å radiation, the initial, excited, and final states are $J=\frac{1}{2}$ states split into $F=0$ and $F=1$ hyperfine levels. The hyperfine splitting, $\Delta\nu=1.2\times10^{10}$/sec, of the $7\,^2S_{1/2}$ level is much greater than the lamp linewidths, so terms with $G\neq G'$ are dropped from Eq. (25). The result of using Eq. (12) in Eq. (25) is then

$$\bar{S}\propto I_{10}+2I_{11}+I_{01}+\{\pm\}\{\pm\}'(I_{11}+I_{01})\cos\theta\cos\theta' + \frac{\{\pm\}\{\pm\}'(I_{11}+I_{01})\sin\theta\sin\theta'}{1+(\mu_0 H\tau/\hbar)^2} \times[\cos(\varphi-\varphi')+\mu_0 H\tau/\hbar\sin(\varphi-\varphi')]. \tag{13}$$

The energies of the $7\,^2S_{1/2}$, $F=1$ levels have been taken as $E_0+m\mu_0 H$ since $g_F=1$ and, for the magnetic fields used in this experiment, the quadratic Zeeman effect contributes less than 0.3% correction to the energy separations of these levels. The maximum crossing signal is seen to occur at $\theta=\theta'=\pi/2$. Using these angles we detected the 3776 Å radiation scattered at $\varphi-\varphi'=\pi/2$ by a beam of Tl atoms in vacuum. The level-crossing signals were also measured at $\varphi-\varphi'=\pi/2$ and $\varphi-\varphi'=\pi$ by detecting the 5350 Å decay radiation to the $6\,^2P_{3/2}$ state. In the later cases Eq. (25) must be modified by defining F', m' as the sublevels of the $6\,^2P_{3/2}$ state. The result has the same dependence on H, τ, and the angles as does Eq. (13), but the relative size of the H-dependent term is somewhat smaller than that in Eq. (13).

In all cases the recorded signals were obtained by modulating and sweeping the magnetic field and phase detecting the scattered light amplitude. A lock-in signal proportional to $d\bar{S}/dH$ was thus recorded, and a modulation correction was applied to find the actual magnetic linewidth from the measured width.[20] [For $B=(\pi\mu_0 g_F\tau)\cdot(P-P$ mod. field$)\ll1$ this is just $1-\frac{3}{4}B^2$.] It should be noted that the values of I_{10}, I_{11}, and I_{01} do not influence the shape of the crossing signal. Another helpful feature in the experiment is that a mixing of a $(\mu_0\tau H/\hbar)/[1+(\mu_0\tau H/\hbar)^2]$ (dispersion) shaped crossing signal into a primarily $1/[1+(\mu_0\tau H/\hbar)^2]$ (Lorentzian) shaped signal (or vice versa) has a noticeable effect on the positions of the derivative-signal maxima (or zeros) but a very small effect on the signal width.[21] This mixing will occur if the θ, θ', $\varphi-\varphi'$ angles are not exactly $\pi/2$ or π. The 3776 Å detection experiment at $\theta=\theta'=\varphi-\varphi'=\pi/2$ was repeated with a 20-mm deep, 20-mm-diam. scattering cell to determine the effects of multiple scattering. At vapor pressures between 10^{-6} and 10^{-5} mm, no linewidth narrowing was observed; between 10^{-5} and 2×10^{-4} mm the signal size decreased rapidly due to depolarizing scattering, but the narrowing, if present at all, was still less than 5%. The lifetimes calculated from the measured linewidths were all within the quoted result of $7.6\pm0.2\times10^{-9}$ sec.

IV. MEASUREMENT OF $A(7\,^2S_{1/2}-6\,^2P_{1/2})/A(7\,^2S_{1/2}-6\,^2P_{3/2})$

Thallium atoms excited to the $7\,^2S_{1/2}$ state will decay to the $6\,^2P_{1/2}$ and $6\,^2P_{3/2}$ levels emitting 3776 and 5350 Å radiation, respectively. The relative probability of making either spontaneous-decay transition is just the ratio of the two transition probabilities per sec. The radiation from each $7\,^2S_{1/2}$ state sublevel will be isotropic and polarized, and if all the sublevels are equally pumped the total radiation will be isotropic and unpolarized. Thus, with equal or unequal pumping rates into the $7\,^2S_{1/2}$ state sublevels, the relative number of 3776 to 5350 Å photons radiated in any direction by a naturally decaying thallium atom will be the desired ratio of the transition probabilities per sec. To measure this relative number of photons from a gas of excited thallium atoms, it is necessary that few collision processes occur during the $7\,^2S_{1/2}$ state spontaneous-decay lifetime of about 10^{-8} sec, and that the trapping of the 3776 Å radiation be corrected for by finding the limiting ratio at low vapor density.

The collision probability can be minimized, the vapor density can be easily controlled, and the two desired spectral lines isolated from the thallium spectrum by measuring the intensity ratio in the fluorescence of a beam of thallium atoms optically pumped to the $7\,^2S_{1/2}$ state. This method was employed in the experiment with the detector at 90° to the incident unpolarized pumping radiation to minimize background radiation into the detector. All radiation other than 3776 Å that could excite the atoms was then easily blocked between the lamp and the scattering gas (with glass) so that only the 3776 and 5350 Å lines were fluoresced by the gas (neglecting the $6\,^2P_{3/2}\rightarrow 6\,^2P_{1/2}$ forbidden transition). Any remaining lamp radiation not blocked by the glass simply added to the instrumental-scattering background seen by the detector. This instrumental scattering was accurately evaluated by using for the scattering gas a beam of thallium atoms that could be blocked by a beam flag. The filters used between the thallium beam and the detector to block one of the lines were absorption filters (Schott UG-5, GG-14, Corning 3-73, 7-51, Wratten

[19] A. Gallagher and A. Lurio, Phys. Rev. Letters **10**, 25 (1963).
[20] H. Wahlquist, J. Chem. Phys. **35**, 1708 (1961).
[21] A. Lurio and R. Novick, Phys. Rev. **134**, A608 (1964).

$K2$-#8) which transmitted 80% to 90% of the desired line and less than 0.1% of the other. No lenses were used between the beam and detector, and the detected radiation was limited to less than a $\pm 12°$ angular spread in all cases and to less than $\pm 5°$ for most of the data. Since the optical density of each filter is small at the desired line and is proportional to the path length through the filter, the filter absorption does not vary more than a small fraction of a percent within these angles. Consequently, the filter transmissions could be calibrated in a Cary spectrometer and checked in the experiment by putting them in series. The $\frac{1}{16}$-in. quartz vacuum window has a transmission that differs by about $\frac{1}{4}\%$ at the two wavelengths.

A phototube sensitivity was necessary to measure accurately the fluorescent intensities from the vapor, but the spectral response of phototubes not only varies greatly between tubes of the same type, it varies considerably across the cathode of each phototube. Consequently, an RCA 5819 phototube (selected for homogeneity of response) was calibrated by exposing a fixed cathode area to a $\frac{1}{2}$-in.-diam. exit aperture of a $1\frac{1}{2}$-in.-radius integrating sphere. The hollow sphere was made of wrinkled aluminum foil, which has virtually identical reflection coefficients at our two wavelengths. The entrance aperture of the integrating sphere was $\frac{3}{4}$-in. square and positioned 90° from the exit aperture. This phototube integrating-sphere detector gave the same response ratio for the 3776 and 5350 Å lines for all angles of less than 30° between the detector axis and light direction, and for widely divergent light. To calibrate the relative response of this detector at the two wavelengths, its response ratio was compared to the response ratio of a lampblack-coated, Eppley thermopile. A grating monochrometer was used to isolate the 3776 and 5350 Å lines from an Osram thallium lamp, and quartz lenses focused the exit slit on the detectors. A water filter was used to block infrared scattering through the monochrometer, and a dichroic mirror was used to make the two line intensities almost equal at the detectors and thus minimize errors due to thermopile nonlinearities and zero shifts. The influences of scattering in the monochrometer and dispersion in the quartz lenses were evaluated and corrected for, and the 3519 and 3529 Å lines were adequately isolated from the 3776 Å line by the monochrometer.

The 4000 Å-blazed monochrometer has $f=4.5$ optics, which in conjunction with the Osram lamps gave an intensity of about $\frac{1}{2}$ μW onto the detectors for each line. In order to measure this intensity accurately with the thermopile, it was operated in vacuum. This increased the absolute sensitivity by about 100% and decreased the drifts to less than 10%, but increased the response time constant to about 10 sec. Slow fluctuations were still serious so the light beam was chopped at a 7.5 sec on 7.5 sec off-rate and the thermopile output, after dc amplification, was phase detected at 1/15 cps. with a 80-sec integration time constant. This slow chopping rate was necessary since the thermopile output dropped off rapidly with increasing repetition rates. Using this method, a sensitivity of about 5×10^{-10} V or 2.5×10^{-9} W of radiation was achieved with the thermopile vacuum chamber thermally insulated from the room and the $\frac{1}{8}$-in.-thick quartz vacuum window isolated from stray air currents. The thermopile linearity was checked with neutral-density filters against phototube linearity and found to be excellent under the above conditions. The response ratio of the phototube to the two lines versus the response ratio of the thermopile was measured with three Osram Tl lamps of different intensity ratio and with two different combinations of lenses. The average ratios 0.797, 0.810, 0.797, respectively, were found in the three cases for the phototube 3776 Å/5350 Å signal ratio divided by the thermopile signal ratio. The effect of the $\frac{1}{8}$-in. quartz vacuum window of the thermopile was also evaluated and found to introduce about 0.3% differential absorption. An Epply lampblack-coated thermopile was used in the experiment, and the manufacturer has measured the reflection coefficients through the visible and found them to be equal within $\frac{1}{4}\%$. (This result is supported by other tests of the reflectivity of lampblack.) Different penetration of the lampblack by the different wavelength radiations could influence the ac response of the thermopile, but at the wavelengths and slow chopping rate used this should introduce negligible error. We thus conclude from the calibration that the integrating-sphere phototube detector has a relative response within the values 0.800 ± 0.015.

The ratio of the 3776 and 5350 Å intensities fluoresced by the beam was measured as a function of beam density with various combinations of the above filters and with several detector arrangements. The results are plotted in Fig. 4 against the total intensity of the beam scattering. At constant lamp intensity, this fluorescent intensity is a roughly linear index of the beam density. Since it is used only as a way of finding the low beam-density limit, lamp ageing or intensity fluctuations cause unimportant small shifts along the abscissa. Fluctuations of beam density and lamp intensity were corrected

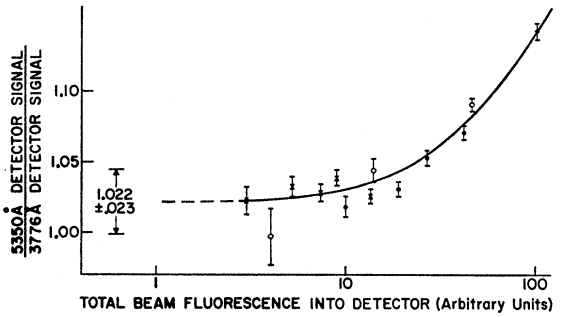

FIG. 4. Relative signal amplitudes from the phototube integrating-sphere detector in the $A(7\,^2S_{1/2}\text{-}6\,^2P_{3/2})/A(7\,^2S_{1/2}\text{-}6\,^2P_{1/2})$ experiment. Each point is the average of eight measurements at each wavelength in one setup. The standard deviations are indicated.

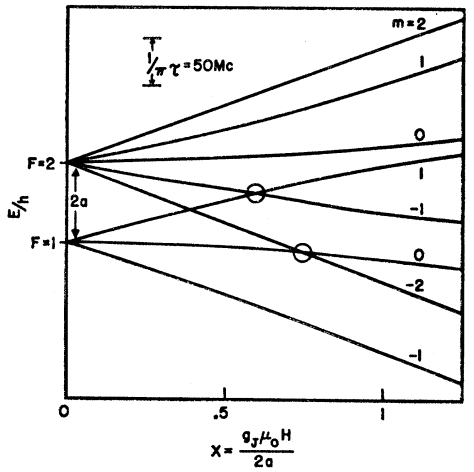

FIG. 5. Energy-level diagram of the $6\,^2D_{3/2}$ state. The detected high-field $\Delta m=2$ crossings are circled (a is arbitrarily shown positive.)

for in the ratio measurements by monitoring the total beam scattering with a second (uncalibrated) phototube placed 180° from the calibrated detector. The limiting ratio, 5350 Å detector signal/3776 Å detector signal $=1.022\pm0.023$, concluded from the data is shown in Fig. 4. To find the equivalent 5350 Å/3776 Å photon ratio we must multiply this by the 3776 Å/5350 Å relative sensitivity of the detector (0.800 ± 0.015) and by the relative energies of the photons. The result is

$$\frac{A(7\,^2S_{1/2}\text{-}6\,^2P_{3/2})}{A(7\,^2S_{1/2}\text{-}6\,^2P_{1/2})}=(1.022\pm0.023)(0.800\pm0.015)\times\frac{5350}{3776}=1.16\pm0.05.$$

V. MEASUREMENT OF THE Tl $6d\,^2D_{3/2}$ STATE LIFETIME AND hfs

The level-crossing technique was also used to measure the $6\,^2D_{3/2}$ state lifetime and hfs.[22] From the energy-level diagram for this state (Fig. 5) it is apparent that a measurement of the magnetic fields at which the two circled high-field, $\Delta m=2$ crossings occur will determine the hfs, but these crossings will not be resolved as can be seen from the natural linewidth, $1/2\pi\tau$, shown in the same figure. The experimental arrangement of angles and polarization was therefore adjusted to optimize the detection of $\Delta m=2$ crossing, i.e., the incident and detected radiation perpendicular to the magnetic field and to each other, and the detecting light analyzed in the transverse plane. The incident 2768 Å radiation was not polarized to avoid loss of intensity, but at the expense of an increase in background. Decay radiation to the $6\,^2P_{3/2}$ state (3529 Å) was detected since the effects of instrumental scattering could thus be minimized and the desired polarization selected without serious intensity loss. 210-cps magnetic-field modulation at the cell was provided by a set of auxiliary coils so that the scattered light signal, $\bar{S}$, could be phase-detected to yield a measurement of $d\bar{S}/dH$. The expected magnetic-field dependence of the scattered radiation has been calculated in Appendix II from Eq. (25) in Appendix I. This $\bar{S}$ [Eq. (28)] and its derivative were evaluated by with an IBM 1620 computer for various values of the parameters a, τ, and R. ($a=6\,^2D_{3/2}$ state dipole coupling constant, $\tau=$lifetime of $6\,^2D_{3/2}$ state, $R=I_0/I_1$ as defined in Fig. 1.)

The effect of the high-field crossing on the calculated $d\bar{S}/dH$ is shown in Fig. 6(a). The positions of the peaks and troughs of the theoretical high-field crossing signals

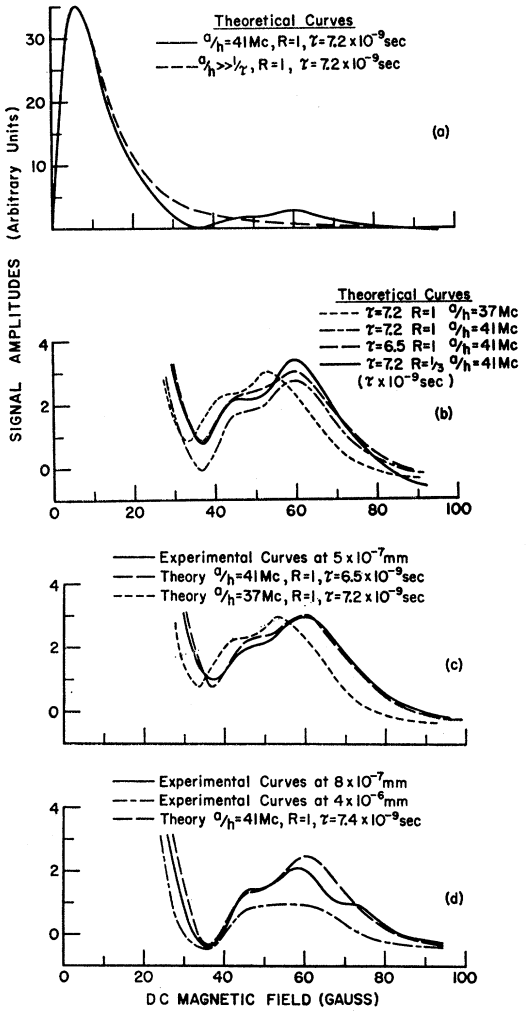

FIG. 6. $6\,^2D_{3/2}$ state high-field level-crossing signals. All signal amplitudes are adjusted to 35 units at the peak of the zero-field crossing signal.

[22] W. Gough and G. Series have recently performed a level-crossing experiment in the Tl $6\,^2D_{3/2}$ state (private communication). Their results, $2|a|/h=84.4\pm3.5$ Mc/sec and $\tau=(5.2\pm0.8)\times10^{-9}$ sec, agree with ours within experimental errors. We are indebted to them for bringing to our attention the R dependence of the signal linewidths.

were found to be fairly insensitive to changes of τ and R, so that $|a|$ could be readily established from the high-field signal curves. This can be seen from the family of $d\bar{S}/dH$ curves plotted in Fig. 6(b), where the only significant differences between the three high-field curves with the same $|a|$ but different τ and R are the amplitudes, but the high-field peaks of the curve with smaller $|a|$ are shifted to lower magnetic field. The values of R and τ used to determine the $|a|$ values lead to a reasonable fit over the entire $d\bar{S}/dH$ curve, only part of which is shown in Fig. 6. In Figs. 6(c) and (d), the data at three cell vapor pressures are compared to computed curves. The effect of multiple scattering on the high-field crossings is primarily to reduce the signals, due to scattering by the noncrossing states. Thus the entire high-field crossing begins to disappear at higher vapor pressure [Fig. 6(d)]. At two lower pressures, the slight effect of multiple scattering could apparently be reasonably well represented by an increase of τ in the theory [Figures 6(c) and (d)]. All the data taken with the cell pressure below 10^{-6} mm agree with those shown and give us the result $|a|/h=41 \pm 2$ Mc/sec.

To evaluate τ from the data, one must consider the effect of the intensity ratio R on the signal shape. The zero-field, $\Delta m=2$ level crossing signal produced by the $6\,^2D_{3/2}$ $F=2$ states is approximately Lorentzian shaped with $g=0.6$, while that produced by the $F=1$ states is also approximately Lorentzian but with $g=1$. Since the ratio R determines the relative amounts of excitation to the $6\,^2D_{3/2}$ $F=1$ and $F=2$ levels, it determines the relative sizes of the contributions to the zero-field crossing signal by these levels. For a lamp without self-reversal, the intensity ratio R of the centers of the $6\,^2P_{1/2}$ state $F=0$ and $F=1$ lines would be $\frac{1}{3}$, but any lamp self-reversal tends to increase this ratio due to the three-times-larger absorption probability from the $6\,^2P_{1/2}$ $F=1$ state. From the computations we find that the zero-field crossing signal follows closely

$$\bar{S} \propto \frac{1}{1+[4\pi\tau g_{\rm eff}(\mu_0/h)H]^2},$$

with the effective g value, $g_{\rm eff}$, varying from 0.72 in the case of an unreversed lamp to 1.0 in the limit of a very strongly self-reversed lamp. The maximum of the detected $d\bar{S}/dH$ occurs almost exactly at $H_{\max}=1/4\pi g_{\rm eff}\tau(\mu_0/h)\sqrt{3}$. The same modulation-correction formulas used in the $7\,^2S_{1/2}$ level-crossing experiment apply here with $B=(2\pi g_{\rm eff}\mu_0\tau)(P-P$ mod. field) for the $\Delta m=2$ crossing case.[20] Barrat[16] has demonstrated and explained the narrowing of zero-field crossing signals due to multiple scattering. The true width must be found by extrapolating the linewidth data to the limit of zero vapor density of scattering atoms. Our results are shown in Fig. 7 for a 1-in.-deep, 1-in.-diam. cell of scattering gas. To determine the lifetime from these

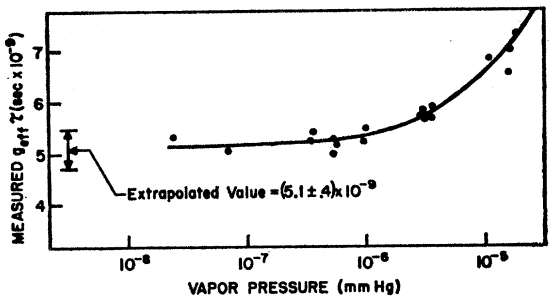

FIG. 7. Measured "Lorentzian" linewidths of the $6\,^2D_{3/2}$ state zero-field level-crossing signals.

results we need $g_{\rm eff}$, or R, for our lamp. A careful fit of the entire $d\bar{S}/dH$ curve to the data determines $g_{\rm eff}$ fairly well, but our data are sufficiently accurate over the entire range to allow us to assert only that $g_{\rm eff}>0.90$ is very unlikely. In addition, $g_{\rm eff}>0.90$ requires an intensity ratio $R=4$ rather than the unreversed ratio $\frac{1}{3}$. This requires extreme self-reversals of both lines; a condition which does not lead to maximum scattering intensities and is therefore unlikely when adjusting our lamp conditions to optimise scattered intensity. Consequently, we will use $g_{\rm eff}=0.82\pm0.1$ for our lamp, with the result that $\tau(6\,^2D_{3/2})=6.2\pm1\times10^{-9}$ sec.

VI. RESONANCE LAMPS USED IN THE EXPERIMENTS

Osram thallium lamps were used exclusively in the $A(7\,^2S_{1/2}$-$6\,^2P_{3/2})/A(7\,^2S_{1/2}$-$6\,^2P_{1/2})$ experiment since repeatability and stability, rather than intensity, were the primary requisites in this case. In the $7\,^2S_{1/2}$ lifetime experiments, Osram lamps were used for preliminary work due to their ease of operation, but a gas-flow lamp of the Cario-Lochte-Holtgreven (CLH) type was used in taking final data since its useful 3776 Å intensity was about five times that of the Osram lamp at average conditions. The Osram lamps were rf excited to prevent intensity modulation, and the power was adjusted to produce the maximum useful intensity. In the CLH lamp, thallium vapor from an oven and counterflowing argon gas were excited by electrodeless rf-discharge. The features of the lamp design followed those developed at the Columbia Radiation Laboratory.[23]

The CLH lamp (with a quartz window) was also used for the 2786 Å pumping radiation of the $6\,^2D_{3/2}$ state experiment. The 2768 Å intensity was about 10^{-2} times the 3776 Å intensity from the same lamp (for average operating conditions in each case). More rf power and a smaller Tl vapor flow from the oven were necessary to maximize the 2768 Å intensity. For both lines, the gas pressure had to be carefully adjusted to prevent ($\sim$5%) oscillations of light intensity at audio frequencies. Once

[23] Columbia Radiation Laboratory Quarterly Progress Report, December 16, 1961 to March 15, 1962 (unpublished). An article describing this lamp by B. Budick, R. Novick and A. Lurio has been submitted for publication to Applied Optics.

TABLE I. Thallium oscillator strengths.

Transitions	$10^2 f_{exp}$	$10^{-7}A_{exp}$	$10^{-7}A_{B\&D}$[a]	$10^{-7}A_{B\&D}$[b]	$10^{-7}A_{Vainshtein}$
$7\,^2S_{1/2}$-$6\,^2P_{1/2}$	13.3 ±0.7	6.25±0.31	2.13	3.3	5.23[c]
$8\,^2S_{1/2}$-$6\,^2P_{1/2}$	1.76 ±0.16	1.78±0.16	0.56	1.7	
$9\,^2S_{1/2}$-$6\,^2P_{1/2}$	0.62 ±0.08	0.78±0.10	0.24	0.90	
$10\,^2S_{1/2}$-$6\,^2P_{1/2}$	···	···	0.12		
$11\,^2S_{1/2}$-$6\,^2P_{1/2}$	0.22 ±0.04	0.31±0.06	···	0.28	
$12\,^2S_{1/2}$-$6\,^2P_{1/2}$	0.13 ±0.03	0.20±0.05	···		
$7\,^2S_{1/2}$-$6\,^2P_{3/2}$	15.1 ±0.7	7.05±0.32	4.00	4.8	6.8[c],8.9[d]
$8\,^2S_{1/2}$-$6\,^2P_{3/2}$	1.36 ±0.14	1.73±0.18	1.08	2.1	
$9\,^2S_{1/2}$-$6\,^2P_{3/2}$	0.48 ±0.05	0.80±0.08	0.47	0.93	
$10\,^2S_{1/2}$-$6\,^2P_{3/2}$	0.30 ±0.03	0.57±0.06	0.25	0.56	
$11\,^2S_{1/2}$-$6\,^2P_{3/2}$	···	···	···		
$12\,^2S_{1/2}$-$6\,^2P_{3/2}$	0.080±0.008	0.16±0.02	···		
$13\,^2S_{1/2}$-$6\,^2P_{3/2}$	0.050±0.005	0.11±0.01	···		
$6\,^2D_{3/2}$-$6\,^2P_{1/2}$	29.0 ±2.2	12.6 ±1.0	12.6	9.7	
$7\,^2D_{3/2}$-$6\,^2P_{1/2}$	7.4 ±0.9	4.4 ±0.5	4.7	3.8	
$8\,^2D_{3/2}$-$6\,^2P_{1/2}$	2.8 ±0.4	1.87±0.30	2.5	2.1	
$9\,^2D_{3/2}$-$6\,^2P_{1/2}$	1.4 ±0.30	0.98±0.22	···	0.73	
$10\,^2D_{3/2}$-$6\,^2P_{1/2}$	0.80 ±0.20	0.58±0.15	···		
$11\,^2D_{3/2}$-$6\,^2P_{1/2}$	0.54 ±0.16	0.40±0.12	···		
$6\,^2D_{3/2}$-$6\,^2P_{3/2}$	4.0 ±0.4	2.20±0.23	2.3	1.9	
$7\,^2D_{3/2}$-$6\,^2P_{3/2}$	0.91 ±0.09	0.76±0.08	0.85	0.71	
$8\,^2D_{3/2}$-$6\,^2P_{3/2}$	0.40 ±0.04	0.37±0.04	0.41	0.29	
$9\,^2D_{3/2}$-$6\,^2P_{3/2}$	0.20 ±0.02	0.19±0.02	···	0.13	
$6\,^2D_{5/2}$-$6\,^2P_{3/2}$	34.6 ±3.5	12.4 ±1.3	13.9	11.4	
$7\,^2D_{5/2}$-$6\,^2P_{3/2}$	8.1 ±0.9	4.2 ±0.5	5.1	4.2	
$8\,^2D_{5/2}$-$6\,^2P_{3/2}$	2.8 ±0.3	1.7 ±0.2	2.4	1.7	
$9\,^2D_{5/2}$-$6\,^2P_{3/2}$	1.5 ±0.2	1.0 ±1	···	0.75	

[a] Calculated from B & D tables.
[b] Calculated directly using B & D wave functions and method.
[c] Without exchange.
[d] With exchange.

conditions were optimized, stable operation could generally be achieved for several hours. The Osram lamp was found to have a quite negligible amount of 2768 Å radiation, even with the usual vacuum jacket replaced by a quartz vacuum jacket.

VII. THALLIUM OSCILLATOR STRENGTHS

We will describe the experimental results on which our table of oscillator strengths (Table I) is based and then compare the remaining oscillator-strength information in the literature to the values in Table I. We will attempt to explain some of the disagreements and to justify our choice of experimental results by discussing plausible sources of error in some of the experiments. The thallium oscillator strengths will then be compared to the prediction of the Vainshtein and the B & D calculations, and the method used to extend the B & D table will be described.

The most accurate absolute value on which the oscillator-strength table can be based is, we believe, the $7\,^2S_{1/2}$ state lifetime reported here. If we average our two measured values of $7.4\pm0.3\times10^{-9}$ sec and $7.6\pm0.2\times10^{-9}$ sec, we then have

$$1.33\pm0.03\times10^8=1/\tau(7\,^2S_{1/2})=A(7\,^2S_{1/2}\text{-}6\,^2P_{1/2})+A(7\,^2S_{1/2}\text{-}6\,^2P_{3/2}). \quad (14)$$

We have measured the ratio of these two transition probabilities per sec, with the result $A(7\,^2S_{1/2}\text{-}6\,^2P_{3/2})/A(7\,^2S_{1/2}\text{-}6\,^2P_{1/2})=1.16\pm0.05$. This ratio has already been measured in two AD experiments and in an intensity-ratio experiment,[3–5] and although two of the results disagree with ours the AD data of Kvater lead to almost the same ratio that we measured. These data were not analyzed by Kvater to establish the best ratio, but this can be readily done by assuming that the relative populations of the $6\,^2P_{1/2}$ and $6\,^2P_{3/2}$ levels are given by a Boltzmann distribution. (Nikinova and Prokofiev have pointed out this information in Kvater's data.)[24] Kvater's data establish the ratio at five Tl vapor pressures between 3.7×10^{-3} and 2.3×10^{-2} mm, and the average of these five ratios is $A(7\,^2S_{1/2}\text{-}6\,^2P_{3/2})/A(7\,^2S_{1/2}\text{-}6\,^2P_{1/2})=1.105$, while the standard deviation of the average is 0.012. We have used the compromise value of 1.13 ± 0.05 to calculate $A(7\,^2S_{1/2}\text{-}6\,^2P_{3/2})$ and $A(7\,^2S_{1/2}\text{-}6\,^2P_{1/2})$ from Eq. (14). The result is presented in Table I with the experimental "maximum" errors compounded by direct addition of the % errors. We have next used the $A(n\,^2S_{1/2}\text{-}6\,^2P_{1/2})/A[(n+1)^2S_{1/2}\text{-}6\,^2P_{1/2}]$, $A(n\,^2D_{3/2}\text{-}6\,^2P_{1/2})/A[(n+1)^2D_{3/2}\text{-}6\,^2P_{1/2}]$, and $A(6\,^2D_{3/2}\text{-}6\,^2P_{1/2})/A(7\,^2S_{1/2}\text{-}6\,^2P_{1/2})$ ratios of Prokofiev and Filippov[25] to establish the $A(n\,^2D_{3/2}\text{-}6\,^2P_{1/2})$ and $A(n\,^2S_{1/2}$-

[24] E. Nikinova and V. Prokofiev, Opt. i Spektroskopiya 1, 290 (1956).
[25] N. Filippov and V. Prokofiev, Z. Physik 85, 647 (1933).

$6\,^2P_{1/2}$) values in Table I from this $A(7\,^2S_{1/2}\text{-}6\,^2P_{1/2})$ value. Similarly the $A(n\,^2S_{1/2}\text{-}6\,^2P_{3/2})/A(7\,^2S_{1/2}\text{-}6\,^2P_{3/2})$, $A(n\,^2D_{3/2}\text{-}6\,^2P_{3/2})/A(7\,^2S_{1/2}\text{-}6\,^2P_{3/2})$, and $A(n\,^2D_{5/2}\text{-}6\,^2P_{3/2})/A(7\,^2S_{1/2}\text{-}6\,^2P_{3/2})$ ratios of Penkin and Shabanova[26] have been used to establish the $A(n\,^2D_{5/2}\text{-}6\,^2P_{3/2})$, $A(n\,^2D_{3/2}\text{-}6\,^2P_{3/2})$, and $A(n\,^2S_{1/2}\text{-}6\,^2P_{3/2})$ values in the table from the $A(7\,^2S_{1/2}\text{-}6\,^2P_{3/2})$ value. The "maximum" errors reported in these experiments have again been compounded by direct addition of % errors. The only ratio for which no error was reported by the authors is $A(6\,^2D_{3/2}\text{-}6\,^2P_{1/2})/A(7\,^2S_{1/2}\text{-}6\,^2P_{1/2})$, which had a negligible standard deviation of the average, and it has been arbitrarily assigned a $\pm 3\%$ margin of error. With the values in Table I thus determined we are prepared to make comparisons with the results of other experiments.

We will first compare our experimental results $1/\tau(6\,^2D_{3/2}) = (16.1\pm 2.6)\times 10^7/\text{sec}$ with the Table I values:

$$A(6\,^2D_{3/2}\text{-}6\,^2P_{1/2}) + A(6\,^2D_{3/2}\text{-}6\,^2P_{3/2}) = (12.6\pm 1.0)\times 10^7/\text{sec} + (2.20\pm 0.23)\times 10^7/\text{sec} = (14.8\pm 1.2)\times 10^7/\text{sec}.$$

The agreement is certainly satisfactory in this case.

We will next consider the absolute oscillator-strength measurements by AD. As has been noted, these values depend on a determination of the Tl vapor pressure as a function of temperature and this was not accurately known until recently. Gurvich[2] has reanalyzed Kvater's data using recent vapor-pressure information and his conclusion is $A(7\,^2S_{1/2}\text{-}6\,^2P_{1/2}) = 5.8\times 10^7/\text{sec}$ and $A(7\,^2S_{1/2}\text{-}6\,^2P_{3/2}) = 6.2\times 10^7$ sec. He notes, however, that the remaining vapor-pressure uncertainty leaves a 0% to +20% uncertainty in these values and they are, respectively, 7% and 11% lower than the values in Table I. Penkin and Shabanova[26] have also found the above values from the same data using still newer vapor-pressure information, but they have apparently not applied it to their own data. An unexplained discrepancy of about 10% may therefore still exist. The absolute oscillator-strength results which are not valid due to erroneous vapor-pressure information are those given by Kuhn,[27] Filippov and Prokofiev,[25] and Kvater.[3,28]

There are two additional values in the literature for the $7\,^2S_{1/2}$ lifetime. One value (10% larger than our result) is a report of results established at our laboratory by Tolnas and Lurio[29] with the double-resonance experiment, but with much smaller signal to noise than was ultimately achieved. The lifetime found by Demtroder[30] is 18% larger than our value; a disagreement which is much greater than the quoted uncertainties. In this experiment, Demtroder measured the phase shift between modulated 3776 Å pumping radiation and the (modulated) radiation fluoresced by thallium vapor. By modulating at frequencies in the range of $1/\tau$, he detected the time the scattered radiation was trapped in the vapor. In the limit of zero vapor pressure, each scattered photon will undergo only one scattering and the trapping time will be the lifetime of the excited state, but all multiple scattering will increase this measured trapping time. Demtroder[31] did not (with thallium) measure over a large range of vapor pressures to establish the limiting trapping time, but he believes that, with his geometry and vapor pressure of about 10^{-5} mm, multiple-scattering did not affect his thallium results. (He did use limiting values for other elements.) This remains, therefore, the most disturbing disagreement amongst the various experimental results.

Stephenson[32] utilized a magnetorotation method, which should be independent of the vapor density, to measure $A(7\,^2S_{1/2}\text{-}6\,^2P_{3/2})$. His conclusion is $A(7\,^2S_{1/2}\text{-}6\,^2P_{3/2}) = (7.00\pm 0.3)\times 10^7/\text{sec}$, but his result is actually $6.14\times 10^7/\text{sec}$ since he used $Z=\frac{4}{3}$, rather than 7/6 as he had intended, in the last step of calculating A from his data. In addition, he uses a formula valid only in the Paschen-Back region, while his measurements were performed at a magnetic field (30 G) which splits the $7\,^2S_{1/2}$ state and $6\,^2P_{3/2}$ state levels by much less than the hfs separations (i.e., in the normal Zeeman-effect region). The usual normal Zeeman-effect-region interpretation[1] would lead to a roughly 40% lower A value from the same data. This corrected result is in considerable disagreement with the A value in Table I, and since the latter result is supported at least within 20% by the above comparisons with Refs. 2, 26, 29, and 30, the result of Ref. 32 is apparently inaccurate.

Hinnov and Kohn[33] have made intensity measurements in flame spectra from which they have evaluated a number of oscillator strengths. From their comparison of their results with accepted values (e.g., in the alkalis) it can be seen that their A values are generally within a factor of 2 of the accepted values. Their thallium results are $A(7\,^2S_{1/2}\text{-}6\,^2P_{3/2}) = 13\times 10^7/\text{sec}$ and $A(7\,^2S_{1/2}\text{-}6\,^2P_{1/2}) = 7.9\times 10^7/\text{sec}$, certainly within a factor of 2 of our values.

Muller[34] measured the total absorption by a column of Tl vapor of the unresolved 3529 and 3519 Å lines from a cell of Tl vapor irradiated by 2768 Å radiation from a Tl lamp. His results, $A(6\,^2D_{5/2}\text{-}6\,^2P_{3/2}) + A(6\,^2D_{3/2}\text{-}6\,^2P_{3/2}) = 1.9\times 10^7/\text{sec}$, is too small by roughly a factor of 8, but a brief analysis is nonetheless called for. Muller assumed that all the $6\,^2D_{3/2}$ and $6\,^2D_{5/2}$ Zeeman levels were equally populated by collisions in the cell, but since this is not too probable it is not clear what proportions of 3529 and 3519 Å absorp-

[26] N. Penkin and L. Shabanova, Opt. i Spektroskopiya 14, 167 (1963) [English transl.: Opt. Spectry. (USSR) 14, 87 (1963)].
[27] W. Kuhn, Kgl. Danske Videnskab. Selskab. Mat. Fys Medd. 7, 1 (1926).
[28] G. Kvater, Zh. Eksperim. i Teor. Fiz. 5, 426 (1935).
[29] E. Tolnas and A. Lurio, Bull. Am. Phys. Soc. 6, 75 (1961).
[30] W. Demtroder, Z. Physik 166, 42 (1962).
[31] W. Demtroder, (private communication).
[32] G. Stephenson, Proc. Roy. Soc. (London) A64, 458 (1951).
[33] E. Hinnov and H. Kohn, J. Opt. Soc. Am. 47, 156 (1957).
[34] F. Muller, Helv. Phys. Acta. 8, 152 (1935).

tions were measured. If, as is quite probable, there was very little collision mixing of the $6\,^2D_{3/2}$ and $6\,^2D_{5/2}$ levels, then he measured primarily $A(6\,^2D_{3/2}\text{-}6\,^2P_{3/2})$ and his result is only 15% low. An additional complication, however, is that the cell vapor pressure was so large ($\sim 10^{-1}$ mm) that the central portion of the lamp 2768 Å line would be reflected from the front of the cell and only the edges of 3519 and 3529 Å lines (with lamp linewidths) would be scattered at the side of the cell towards the absorbing column of gas. It is, therefore, difficult to interpret the data.

A number of relative oscillator-strength measurements must now be considered. As mentioned above, there are two additional experiments which measured $A(7\,^2S_{1/2}\text{-}6\,^2P_{3/2})/A(7\,^2S_{1/2}\text{-}6\,^2P_{1/2})$; one by AD and the other from 5350 Å/3776 Å intensity ratio in lamp radiation. The AD measured ratio[5] is 0.95, as opposed to the value 1.13 ± 0.05 which we used. This AD value is an average of the ratios at four Tl vapor pressures between 3.5×10^{-3} and 3.0×10^{-2} mm, and these ratios have such a large vapor-pressure dependence that the values at the highest and lowest pressures are 8% lower and 12% higher, respectively. (All the ratios are also 3.5% too low due to the inaccuracy in the 1928 value of hc/k.) Since the AD theory predicts no such vapor-pressure dependence of the ratio, and since Kvater[3] did not find such an effect, some anomalous effects apparently influenced their results. Vonweiler[4] measured the 5350 Å/3776 Å intensity ratio of the Tl lamp radiation in the limit of low Tl vapor pressure in the lamp. He thus compensated for 3776 Å radiation trapping in a similar manner to that which we employed, but the question of whether or not the Tl atoms decayed spontaneously or partially by collision remains. The major problem, however, is the calibration of the detector. He utilized a tungsten lamp to calibrate a spectrographic detector, but the lamp-radiation temperature was apparently determined by calculation rather than by calibration against black-body radiation. This lamp calibration, slight instrumental scattering in the spectroscope, or other complications mentioned in the paper could easily have produced the small difference between his result, $A(7\,^2S_{1/2}\text{-}6\,^2P_{3/2})/A(7\,^2S_{1/2}\text{-}6\,^2P_{1/2})=0.91$, and our ratio.

The magnetorotation measurements of Kuhn do not yield absolute oscillator strengths due to the vapor-pressure problem, but one might expect his relative values to be significant. From Kuhn's results,[27] $A(7\,^2S_{1/2}\text{-}6\,^2P_{1/2})/A(6\,^2D_{3/2}\text{-}6\,^2P_{1/2})=0.43$ as opposed to the value 0.497 used from Filippov and Prokofiev's AD experiment. Kuhn, however, operated with a rather inhomogeneous magnetic field near 5.5×10^3 G, which is in the intermediate field region for the Tl $6\,^2P_{1/2}$ and $7\,^2S_{1/2}$ levels. Since he used Pashen-Back region formulas to analyze his data, the ratio of A values is not valid without corrections for hfs.

There remains in the literature several AD-measured oscillator-strength ratios which were measured later and more accurately by Penkin and Shabanova.[26] These are

$$\frac{A(6\,^2D_{5/2}\text{-}6\,^2P_{3/2})+A(6\,^2D_{3/2}\text{-}6\,^2P_{3/2})}{A(7\,^2D_{5/2}\text{-}6\,^2P_{3/2})+A(7\,^2D_{3/2}\text{-}6\,^2P_{3/2})}\cong 2.7$$

from Ref. 25, while the value used from Ref. 26 is 2.9 ± 0.3. Also,

$$A(6\,^2D_{5/2}\text{-}6\,^2P_{3/2})/A(6\,^2D_{3/2}\text{-}6\,^2P_{3/2})=6.0\pm0.5\,,$$

and

$$\frac{f(7\,^2S_{1/2}\text{-}6\,^2P_{3/2})}{f(6\,^2D_{5/2}\text{-}6\,^2P_{3/2})+f(6\,^2D_{3/2}\text{-}6\,^2P_{3/2})}=0.37\pm0.02$$

from Ref. 28, while the values used from Ref. 26 are 5.65 ± 0.35 and 0.39 ± 0.02, respectively. The agreement is quite satisfactory in all three cases.

Additional thallium oscillator-strength measurements we have found in the literature are $A(n\,^2P_{3/2}\text{-}7\,^2S_{1/2})/A(n\,^2P_{1/2}\text{-}7\,^2P_{1/2})$ ratios from intensity-ratio measurements of Vonweiler,[4] and $[f(n\,^2D_{5/2}\text{-}6\,^2P_{3/2})+f(n^2\,D_{3/2}\text{-}6\,^2P_{3/2})]/f(7\,^2S_{1/2}\text{-}6\,^2P_{3/2})\,(10\leq n\leq 15)$ ratios measured by Penkin and Shabonova.[26] These ratios supply additional information, but were not used here since no absolute oscillator strengths could be established from them.

As noted in the introduction, the atomic transition probabilities are not precisely equivalent to single-electron transition probabilities due to the configurational mixing. We do not yet have enough information to calculate the amount of configuration mixing in the thallium states, but the information that is available indicates that the mixing probably causes less than 30% correction to the single-valence-electron transition probabilities. The best indication of this is simply the good agreement between the experimental A values and the approximately calculated single-electron A values (to be presented below). Another source of mixing information is the $6\,^2P_{1/2,3/2}$ hfs, from which the most probable magnitude of $6s7s6p$ mixing into the $6s^26p$ configuration can be estimated to be in the range of 10% (see discussion of hfs). From the relations between the amount of $6sNsnl$ mixing into the various $6s^2nl$ states, it then follows that the mixing probably produces considerably less than a 30% alteration in the transition probabilities to the $6\,^2P_{1/2,3/2}$ states. An additional effect of the configuration interaction is to make the ionization energy of each atomic n^2L_J state smaller than that of the single-valence-electron nl state. Since the theories depend on the measured ionization energies for the evaluation of the single-electron functions, this causes further error in calculating the transition probabilities. With these reservations we will compare the calculated single-electron A value directly to the experimental values in Table I.

Single-electron transition probabilities are propor-

tional to

$$\sigma^2 \equiv \frac{1}{4l^2-1}\left[\int_0^\infty R_i r R_f dr\right]^2,$$

where R_i/r and R_f/r are the radial functions of the initial and final states of the electron. When the valence electron is being considered, the major contribution to this integral occurs outside the core, where the field is Coulombic. Noting this, Bates and Damgaard[6] have devised an approximate method for evaluating the integral by using radial functions modeled after the radial functions of hydrogen. Since the values of the R at large r are of primary interest, the functions used are

$$R_{n^*,l} = N_{n^*,l} e^{-r/n^*}(2r/n^*)^{n^*}\left(1+\sum_{t=1}^{\infty} a_t r^{-t}\right),$$

where $N_{n^*,l}$ is the normalization constant, $n^* = 1/\sqrt{E_{\text{Ionization}}}$, the a_t are given by the hydrogenic recursion formula with n^* replacing n, and E and r are in atomic units. When n^* is nonintegral, the series does not terminate as it does for hydrogen, and $R(r)$ is infinite. B & D handled this difficulty by including in the above integrand $R_i r R_f$ only the terms proportional to $\exp[-r/n^*_i - r/n^*_f]r^c$ with $c \geq 2$. Using this method, B & D compiled a table of $\sigma(n^*_l, n^*_{l-1}, l)$ values, but to lighten the load of hand calculations they calculated only the σ integrals for which $n^*_l = l+1, l+2, \cdots$ (i.e., for which $R_{n^*,l}$ is an exact hydrogenic solution). They suggest that σ values for transitions with n^*_l not integrals should be found by interpolation or extrapolation from the calculated values. The thallium A values we find using these tables are presented in the fourth column of Table I. To find the p-d transition probabilities, the tables had to be extrapolated to n^*_d values -0.1 beyond the lowest values in the table, while the tables had to be extrapolated beyond $n^*_p = 2.0$ to $n^*_p = 1.50$ and 1.63 to find the s-p transition probabilities. These extrapolations can be made without introducing serious ambiguity, using the extrapolation method suggested by B & D.

The values in the fifth column of Table I were calculated using the B & D method, but without reference to their tables. Neither n^*_i nor n^*_f were integers in these transitions, but the formal B & D method was still used. i.e., only terms proportional to $\exp[-r/n^*_i - r/n^*_f]r^c$ with $c \geq 2$ were included in $R_i r R_f$, and the normalization constant formula of B & D was used for all the functions (it is defined for $n^* - l > 0$). It can be seen that the B & D transition probabilities in columns 4 and 5 of the table differ by about 20% for the d-p transitions, but by factors of 2 to 3 for most of the s-p transitions. To verify that the larger differences were due to the large extrapolation required for the s-p transitions, we have calculated σ^2 for a number of s-p transitions within the table, with both n^*_i and n^*_f nonintegral, and compared these to the interpolated values using the B & D tables. All regions of the tables were not checked, but the σ^2 found by the two methods agreed within 20% for all the transitions tested. This agrees with the observations of B & D (pp. 105–106 of Ref. 6) and is certainly to be expected since the directly calculated σ becomes identical to the σ in the table when n^*_p takes on the next higher and lower integral values. Since the tables extend only to $n^*_l = l+1$, this argument no longer applies when $n^*_l < l+1$, and one reason for the inaccuracy of the extrapolation becomes clear when the extrapolation method is considered. B & D have defined $\mathcal{G}$ by the relation:

$$\sigma(n^*_l, n^*_{l-1}, l) = \frac{3n^*_l}{2}\left[\frac{n^{*2}_l - l^2}{4l^2-1}\right]^{\frac{1}{2}} \mathcal{G}(n^*_l, n^*_{l-1} - n^*_l, l).$$

The method of extrapolation suggested by B & D is to extrapolate $\mathcal{G}(n^*_l, n^*_{l-1} - n^*_l, l)$ holding $n^*_{l-1} - n^*_l$ and l constant. Since $\mathcal{G}$ varies slowly when n^*_l and n^*_{l-1} are varied in this manner with $n^*_l \geq l+1$, the extrapolation usually consists of changing $\mathcal{G}$ slightly from its value when $n^*_l = l+1$. However, $\sigma(l, n^*_{l-1}, l)$ is generally finite, so that $\mathcal{G}$ must approach ∞ as $n^*_l \to l$. Thus the suggested extrapolation of $\mathcal{G}$ must become inaccurate for n^*_l less than some value between $l+1$ and l. B & D suggested the use of extrapolation as far as $n^*_l = l+0.5$ (p. 107 of Ref. 6), but comparison with the calculated s-p and p-d transitions probabilities of thallium presented here indicates that the extrapolated σ will usually disagree considerably from the calculated σ for n^*_l less than about $l+0.9$. B & D have described the interpolated and extrapolated values as only approximations to the correct predictions of their method (pp. 105–106 of Ref. 6), and they have suggested that the method should be more accurate for less tightly bound states. Comparing columns 3, 4, and 5 of Table I, it can be seen that the directly calculated thallium A values are in far better agreement with the experimental values for the s-p transitions, while columns 4 and 5 are both in reasonable agreement with the experimental p-d transition probabilities. This appears to justify considering the directly calculated values to be the preferred results of the B & D theory.

With the exception of the $7\,^2S_{1/2}$-$6\,^2P_{3/2}$ and $7\,^2S_{1/2}$-$6\,^2P_{1/2}$ transition probabilities, the average disagreement between the experimental and directly calculated B & D values is only 15%, and the maximum disagreement is only 30%, for transitions in Table I. The B & D predictions for $A(7\,^2S_{1/2}$-$6\,^2P_{3/2})$ and $A(7\,^2S_{1/2}$-$6\,^2P_{1/2})$ are, respectively, 35% and 50% too small, but Vainshtein's results for those two transition probabilities are an average of only 15% from the experimental values. Since Vainshtein's method also assumes a single configuration, it appears that the thallium transition probabilities are not greatly influenced by configuration interaction. The fact that the B & D method does not give accurate predictions for the $7\,^2S_{1/2}$ to $6\,^2P_{1/2}$ and $6\,^2P_{3/2}$ transitions is consistent with their assumption

that the theory is less accurate for strongly bound states. The $7s$ to $6p$ transitions involve tightly bound initial and final states, and as a result the regions of small r are more important for these transitions than for the remaining thallium transitions.

VIII. $6d\,^2D_{3/2}$ STATE HYPERFINE STRUCTURE

To the extent that configuration interaction can be neglected, the $6\,^2D_{3/2}$ state of thallium arises from a (core) $6s^26d$ configuration, and its hfs is due entirely to the $6d$ electron. The dipole coupling constant a_J of a single electron may be calculated using the Fermi-Segrè formula with relativistic, screening, and nuclear-penetration corrections[35]:

$$a_J \simeq \frac{g_I L(L+1) F_r(J,Z_i)\delta W_0 m}{J(J+1)(L+\frac{1}{2})Z_i H_r(Z_i,L)M}(1-\delta)(1-\epsilon), \quad (15)$$

where δW_0 is the fine-structure separation, F_r and H_r are tabulated relativistic correction factors, and Z_i is the "effective nuclear charge" (due to the screening) and is usually taken as $Z-10$ for d electrons. δ and ϵ are corrections due to the finite nuclear size and may be neglected for D states. Equation (15) and the familiar relation for the hfs intervals predict for the Tl $6\,^2D_{3/2}$ state

$$\Delta\nu/2h = a/h = 42\times10^6/\text{sec}.$$

The agreement with our experimental result, $|a|/h = 41\pm2$ Mc/sec, is thus excellent if one assumes a is positive as Eq. (15) predicts. We find this result very surprising since the hfs of the $6p^2P_J$ state of Tl I and of the $np\ ^2P_J$ and $nd\ ^2D_J$ states of structurally similar Pb II are strongly influenced by configuration interaction, and we would expect the Tl I $6d^2D_J$ state hfs to be altered for the same reason.

Configuration interaction causes the mixing of different configurations with the same L, S, J, and parity. This mixing often has a large influence on the hfs of states with small hyperfine interactions since they are sensitive to small amounts of mixing with configurations that have large hyperfine interactions. In the $6\,^2P_{1/2,3/2}$ states of thallium, a small amount of the $6s7s6p$ configuration (and smaller amounts of the other $6sns6p$ configurations) mixes into the $6s^26p$ configuration. Since the hyperfine interactions of the $6s$ electrons cancel in the $6s^26p$ configuration, the $6s7s6p$ configuration has a much larger hyperfine interaction and the mixing consequently has a noticeable effect on the $6\,^2P_{1/2,3/2}$ hfs. That this is the correct explanation of the observed hfs values seems fairly certain since Schwartz's configuration-interaction theory has been adequate to explain the hfs anomaly in the Tl $6\,^2P_{1/2,3/2}$ states using $6sns6p$ mixing.[13] We thus expect to find $6s7s6d$ and $6s6p^2$ configurations mixing into the Tl $6\,^2D_{3/2,5/2}$ states, and in this case the small hyperfine interactions of the $6s^26d$ configuration should make the hfs sensitive to very small amounts of mixing.

No wave functions are yet available from which the mixing coefficients might be evaluated, but Koster's success in calculating the hfs of the $4\,^2P_{1/2,3/2}$ states of Ga using Hartree functions and configurational mixing indicates that Hartree functions, when available, may also be sufficient to explain the thallium hfs. The hfs of the Tl $6\,^2P_{1/2,3/2}$ states are expressed in terms of the mixing coefficients of the $6sns6p$ configurations into the $6s^26p$ configuration by Koster's equations, so we have calculated the hfs of the $6\,^2D_{3/2,5/2}$ states in terms of the mixing coefficients of the $6sns6d$ and $6s6p^2$ configurations into the $6s^26d$ configuration. This calculation is presented in Appendix III, where the $6s$, $7s$, $6p$, and $6d$ state dipole coupling constants have been estimated from thallium hfs and fine-structure data, so that the hfs can be expressed directly in terms of the mixing coefficients.

The hfs of the $6\,^2P_{3/2}$ state of Tl is considerably altered by the mixing, so the $6\,^2P_{1/2,3/2}$ hfs can be used as a sensitive test of the mixing coefficients, α_1 of the $6s7s(^3S_1)6p$ configuration and α_2 of the $6s7s(^1S_0)6p$ configuration into the $6s^26p$ configuration. In order to estimate the sensitivity of the $6\,^2D_{3/2,5/2}$ states hfs as a test of the $6s^26d$ configuration mixing coefficients, the probable magnitudes of these coefficients will now be estimated from the mixing of the $6\,^2P_{1/2,3/2}$ of Tl I and the $n\,^2D_{3/2,5/2}$ states of Pb II.

The approximate values found for a_s, S, and σ in Appendix III can be used in the Koster's Eq. (20) to establish one condition on the mixing coefficients α_1 and α_2 of thallium. This is $4.75 = -120\alpha_1^2 + 78\alpha_1 + 175\alpha_1\alpha_2$, and although this is not enough information to establish α_1 and α_2, we may note that Koster found $\alpha_1 = 0.03$, $\alpha_2 = -0.10$ for the equivalent $4s5s4p$ mixing coefficients into the $4s^24p$ configuration of Ga, and values at least as large as those appear likely for Tl judging from this condition. We may also note from Koster's Eqs. (32)–(37) that the largest contribution to α_2 is from a matrix element of electrostatic interaction between the $6s$ and $7s$ electrons (in the Tl case) and the core states ($\sum' N_{n'l',m'i}$ in Koster's notation). This same matrix element will cause the largest contribution to the mixing coefficient d_2 into the Tl $6s^26d$ configuration, and thus $|d_2|$ on the order of 0.1 may be expected. d_1 is determined primarily by a matrix element involving $6d$ with $6s$ and $7s$ interaction $N_{6d,2}$ in place of the $6p$ with $6s$ and $7s$ interaction $N_{6p,1}$ which causes most of α_1. Thus $|d_1| < |\alpha_1|$ may be expected with $|d_1|$ probably on the order of 0.01. The estimate of $|d_3|$ is even more rough since we most rely on the hfs of the $n\,^2D_J$ state of Pb II. In Pb II the $6s6p^2\,^2D_{3/2,5/2}$ states are bound and their hfs, as well as those of the $n\,^2D_J$ states, have been measured. Consequently, it can be seen that the magnitudes and signs of the $n\,^2D_{3/2,5/2}$ hfs are consistent with large amounts of $6s6p^2$ configuration mixing. Some $(6s6p^2)^2D_J$ mixing in Tl I thus appears quite likely, and

[35] H. Kopferman, *Nuclear Moments* (Academic Press Inc., 1958) Sec. 26, p. 26; Sec. 27.

aside from the possibility of coincidental cancellations there is no reason to expect $|d_3|$ to be much less than $|d_2|$.

From these estimates and Eq. (36), one might expect the mixing contributions to the $6\,^2D_{3/2,5/2}$ state hfs to be larger than the contribution from the $6s^26d$ configuration, and the possibility that $a(6\,^2D_{3/2})$ is negative cannot be discarded. It certainly does appear that the agreement of $|a(6\,^2D_{3/2})|$ with the prediction of the Fermi-Segrè formula is a coincidence. In addition, if the estimated magnitudes of the mixing coefficients are correct, then it will be necessary to calculate the coefficients very accurately to explain the $6\,^2D_{3/2}$ state hfs, since considerable cancellation is occurring in Eq. (36) (a difficulty which will probably recur for many of the $n\,^2D_{3/2,5/2}$ states).

ACKNOWLEDGMENTS

We wish to thank Edwin Tolnas for developing most of the apparatus used in the double-resonance experiment, and for performing much of the work on that experiment. We are grateful to A. Willner for programming, for the IBM 1620 computer, the calculated $6\,d^2D_{3/2}$ state level-crossing signals, and to R. Holohan for his frequent assistance in the laboratory.

APPENDIX I

It can be verified[36] that the average intensity of resonance fluorescence $\bar{S}$, under excitation by a radiation field with power density $I(\omega)$ and propagating in the x direction is:

$$\bar{S}=\int_0^\infty d\omega I'(\omega)\bar{S}(\omega)\,, \tag{16}$$

where

$$I'(\omega)=\int_{-\infty}^{\infty} dv_x n(v_x) I\left(\omega-\frac{v_x\omega}{c}\right)$$

is the effective field exciting the atoms, $n(v_x)$ is the number of scattering atoms with velocity v_x, and $\bar{S}(\omega)$ is the average fluorescent power of one atom excited by a monochromatic wave of unit intensity and angular frequency ω. This result is independent of the form of the lamp $E(t)$, or the amount of coherence of the lamp radiation field. It arises essentially from the fact that the interference of the scattered radiation-field amplitudes at different frequencies cannot lead to a contribution to the average scattered radiation. It should be emphasized that this result applies to the average intensity, where the averaging is performed over times much longer than the lifetime of the excited state.

The resonance fluorescence under monochromatic wave excitation may be calculated by taking the limit as γ approaches zero of the scattering of the following electric vector:

$$\mathbf{E}(t)=\mathbf{f}\gamma^{1/2}\exp[-(\tfrac{1}{2}\gamma t+i\omega t)] \quad \text{for } t\geq 0,\quad \mathbf{E}(t)=0 \text{ for } t<0,$$

where $\mathbf{f}$ is a unit vector which describes the polarization and $E(t)$ has been normalized to

$$\int_{-\infty}^{\infty}\mathbf{E}(t)\cdot\mathbf{E}^*(t)dt=1\,.$$

Franken[18] has calculated the total scattered power for the same $E(t)$ except for the coefficient. (He uses $E_0/2$ where we have $\sqrt{\gamma}$.) Consequently, we may use his result [Eq. II, (5) without the integration over ω] with $E_0/2$ replaced by $\sqrt{\gamma}$. This result is

$$S_\omega=\gamma\sum_{\substack{mm'\\ \mu\mu'}} B_{\mu\mu' mm'}\int_0^\infty \frac{dt\exp(-i\omega_{\mu\mu'}t-\Gamma t)\{\exp(i\omega_{\mu\mu'}t-2\lambda t)-\exp[i(\omega_{\mu m}-\omega)t-\lambda t]-\exp[i(\omega-\omega_{\mu' m})t-\lambda t]+1\}}{(\omega_\mu-\omega+i\lambda)(\omega_{\mu'}-\omega-i\lambda)}\,, \tag{17}$$

where $B_{\mu\mu' mm'}=kf_{m\mu'}f_{\mu m}g_{m'\mu}g_{\mu' m'}$, $\lambda=\gamma/2-\Gamma/2$, $\Gamma=1/\tau$, and k is an unimportant proportionality constant. Evaluating the time integral, this becomes:

$$S_\omega=\sum_{\substack{mm'\\ \mu\mu'}}\frac{B_{\mu\mu' mm'}}{\Gamma+i\omega_{\mu\mu'}}\left(\frac{1}{i(\omega_{\mu' m}-\omega)-\lambda}-\frac{1}{i(\omega_{\mu m}-\omega)+\lambda}\right). \tag{18}$$

The limit $\gamma\rightarrow 0$ may be taken in Eq. (18) to give the total fluorescent energy due to the monochromatic wave of frequency ω and unit total energy. This is also clearly the average fluorescent power due to a monochromatic wave of unit average power:

$$\bar{S}(\omega)\equiv\lim_{\gamma\rightarrow 0}S_\omega=\sum_{\substack{mm'\\ \mu\mu'}}\frac{B_{\mu\mu' mm'}}{\Gamma+i\omega_{\mu\mu'}}\left(\frac{1}{i(\omega_{\mu' m}-\omega)-\frac{1}{2}\Gamma}-\frac{1}{i(\omega_{\mu m}-\omega)+\frac{1}{2}\Gamma}\right). \tag{19}$$

We can use Eq. (19) in Eq. (16) to calculate the expected fluorescence under excitation by a typical resonance lamp. Equation (16) may be evaluated for $I(\omega)$ representing only one lamp line at a time and the result summed

[36] A. Gallagher, thesis, 1964, Columbia University, New York, N. Y.

over all the lamp lines. Since we expect a typical line of a resonance lamp to have a Gaussian power density, and the Gaussian velocity distribution, $n(v_x)$, merely makes $I'(\omega)$ a slightly wider Gaussian than $I(\omega)$, we will evaluate the scattering of a radiation field with the Gaussian power density, $I'(\omega)=\exp-[(\omega-\omega_0)/\Delta]^2$. With this $I'(\omega)$, and $\bar{S}(\omega)$ from Eq. (19), Eq. (16) becomes

$$\bar{S}=\sum_{\substack{\mu\mu'\\ mm'}}\frac{B_{\mu\mu' mm'}}{\Gamma+i\omega_{\mu\mu'}}R_{\mu\mu' m}(\omega_0)\,, \tag{20}$$

where

$$R_{\mu\mu' m}(\omega_0)=\frac{-1}{2\pi}\int_{-\infty}^{\infty}dye^{-y^2}\left[\frac{1}{a+i(y+y_\mu)}-\frac{1}{-a+i(y+y_\mu)}\right],\quad(\omega-\omega_0)/\Delta=y,\quad\Gamma/2\Delta=a,\quad(\omega_0-\omega_{\mu m})/\Delta=y_\mu\,.$$

Following Mitchel and Zemansky,[1] or Bitter[37]:

$$\begin{aligned}-\frac{i}{2\pi}\int_{-\infty}^{\infty}dy\frac{e^{-y^2}}{-a+i(y+y_\mu)}&=-\frac{F(y_\mu)}{\sqrt{\pi}}+ay_\mu e^{-y_\mu^2}+\frac{ia}{\sqrt{\pi}}(1-2y_\mu F(y_\mu))\,,\\ \frac{i}{2\pi}\int_{-\infty}^{\infty}dy\frac{e^{-y^2}}{a+i(y+y_{\mu'})}&=\frac{F(y_{\mu'})}{\sqrt{\pi}}-ay_{\mu'}e^{-y_{\mu'}^2}-\frac{i}{2}e^{-y_{\mu'}^2}+\frac{ia}{\sqrt{\pi}}(1-2y_{\mu'}F(y_{\mu'}))\,,\end{aligned} \tag{21}$$

where

$$F(y)=e^{-y^2}\int_0^y e^{x^2}dx$$

varies between 0 and about 0.5. $F(y)$ is a tabulated function so that $R_{\mu\mu' m}(\omega_0)$ can be exactly evaluated for all values of the parameters, but it is useful to consider the approximation when $\Gamma/\Delta\ll1$ since this ratio is less than 0.05 in most cases. In addition, most of the $\mu\mu'$ crossing effect occurs when $\omega_{\mu\mu'}<3\Gamma$, so the approximation $y_{\mu'}-y_\mu=\omega_{\mu\mu'}/\Delta\ll1$ will also be taken. $F(y)$ and e^{-y^2} then may be expanded to give:

$$\begin{aligned}F(y_{\mu'})-F(y_\mu)&\cong(y_{\mu'}-y_\mu)F'(y_\mu)=(\omega_{\mu\mu}/\Delta)F'(y_\mu)\,,\\ y_\mu e^{-y_\mu^2}-y_{\mu'}e^{-y_{\mu'}^2}&\cong(\omega_{\mu\mu'}/\Delta)(1-y_\mu^2)e^{-y_\mu^2}\,,\\ 1-y_{\mu'}F(y_{\mu'})-y_\mu F(y_\mu)&\cong1-2y_\mu F(y_\mu)-(\omega_{\mu\mu'}/\Delta)(F(y_\mu)+y_\mu F'(y_\mu))\,,\\ e^{-y_\mu^2}+e^{-y_{\mu'}^2}&\cong2e^{-y_\mu^2}+(2\omega_{\mu\mu'}/\Delta)y_\mu e^{-y_\mu^2}\,.\end{aligned} \tag{22}$$

With these approximations and F, F', and y evaluated at y_μ, Eq. (20) becomes:

$$R_{\mu\mu' m}(\omega_0)\cong\frac{i\omega_{\mu\mu'}}{\Delta}\left[\frac{F'}{\sqrt{\pi}}+a(1-y^2)e^{-y^2}\right]-\left(\frac{2aF'}{\sqrt{\pi}}-e^{-y^2}\right)-\left[\frac{\omega_{\mu\mu'}}{\Delta}-ye^{-y^2}+\frac{2a}{\sqrt{\pi}}(F+yF')\right]. \tag{23}$$

When $\omega_{\mu m}$ and $\omega_{\mu' m}$ are well inside the line $y_\mu\ll1$, $R_{\mu\mu' m}(\omega_0)\cong1$, and the crossing signal is the same as for $\rho(\omega)=1$. When $\omega_{\mu m}$ and $\omega_{\mu' m}$ are well outside the line $y\ll1$, $F'(y)\to0$, $F(y)\to1/2y$, and

$$R_{\mu\mu' m}(\omega_0)\cong\frac{-\omega_{\mu\mu'}}{\Delta}\frac{2aF(y_\mu)}{\sqrt{\pi}}\cong\frac{-\omega_{\mu\mu'}}{\Delta}\frac{1}{\sqrt{\pi}}\frac{\Gamma}{\omega_{\mu m}-\omega_0}\,. \tag{24}$$

When the two states cross outside the Gaussian line, the crossing signal is seen to be attenuated by somewhat more than $(\Gamma/\Delta)^2$. If one allows the Gaussian $\rho(\nu)$ to drop only to

$$\frac{\Gamma\Delta}{2\sqrt{\pi}}\frac{1}{\Gamma^2+(\omega-\omega_0)^2}$$

on the wings, then there will be an additional contribution of $\Gamma\Delta/2\pi^{1/2}(\omega_{\mu m}-\omega_0)^2$ to $R_{\mu\mu' m}(\omega_0)$ from the intensity remaining at $\omega=\omega_{\mu m}$. This latter contribution will be the larger one, but for $\omega_{\mu m}-\omega_0\geq3\Delta$ and $\Gamma/\Delta\leq1/30$ even this term is smaller than 1×10^{-3}.

Thus the fluorescence from a pair of states crossing well within a line is the same as that from white light with the same $I(\omega)$ as the center of the line, whereas the crossing signal from a pair of states well outside the line is essentially the size of the $I(\omega)$ remaining in the frequency neighborhood of the crossing. For an ordinary resonance-lamp line, the latter signal is quite negligible once the crossing is a few Doppler widths outside the line.

By thus evaluating the average scattering separately for each Gaussian-shaped lamp line, multiplying the result by the relative intensity of the line, and summing over all lines we have the result which can be applied to

[37] J. Bitter, Massachusetts Institute of Technology Research Laboratory for Electronics Technical Report No. 292 (1955) (unpublished).

the experiments:

$$\bar{S}=\sum_{\substack{F,m,F',m'\\G,n,G',n'}}\frac{I_{FG}}{\Gamma+i\omega_{G,n;G',n'}}f_{G,n;F,m}f_{F,m;G',n'}\times g_{G',n';F',m'}g_{F',m';G,n}\delta(\omega_{FG};\omega_{FG'}),\quad(25)$$

where I_{FG} is the relative intensity, at its center, of the $G\rightarrow F$ hfs line of the lamp. The ground-state sublevels have been labeled by F, m; the excited states sublevels by G, n and G', n', and the final state sublevels by F', m'. The δ symbol has been included to indicate that only values of G' for which $|\omega_{FG'}-\omega_{FG}|\ll\Delta$ are to be included in the sum. (The more general condition would be that only values of G', n' for which $|\omega_{F,m;G,m}-\omega_{F,m;G',n'}|\ll\Delta$ be included in the summation, but the small magnetic fields used in the experiments reported here split the Zeeman levels by much less than $\hbar\Delta$ and the value of G' only is significant.)

APPENDIX II

We will calculate the expected average scattering in the $6\,^2D_{3/2}$ state level-crossing experiment by applying Eq. (25) to the excitation from a $L=1$, $J=\frac{1}{2}$ ($S=\frac{1}{2}$) state to a $L=2$, $J=\frac{3}{2}$ excited state with spontaneous decay to a $L=1$, $J=\frac{3}{2}$ state. The nuclear spin is $\frac{1}{2}$ and the hfs of the initial and final states are much greater than that of the excited state being investigated (Fig. 1). Consequently, we will use the correct energies and eigenfunctions of the $6\,^2D_{3/2}$ state in the presence of a dc magnetic field, but leave the initial and final states diagonal in F, m representation.

Since the magnetic moments of the two natural isotopes of Tl (70% Tl^{205}, 30% Tl^{203}) differ by only 1% and the accuracy of this $|a|$ determination was only $\pm5\%$, we will assume only one a in the theory. Since $I=\frac{1}{2}$, the $6\,^2D_{3/2}$ state eigenfunction may be calculated exactly, in terms of the F, m eigenfunctions, with the Breit-Rabi equation. The result is given for an arbitrary J and g_J in Ref. 21 ($J=\frac{3}{2}$, $g_J=0.4$ in this case).

The 2768 Å radiation will be composed of only two resolved hfs lines for each isotope, since the $6\,^2D_{3/2}$ state hfs (about 80 Mc/sec) is smaller than the lamp linewidth but the $6\,^2P_{1/2}$ state hfs (about 2.1×10^4 Mc/sec) is larger than the lamp linewidth. Consequently, $\delta(\omega_{FG},\omega_{FG'})=1$ in Eq. (25) and the relative line intensities may be labeled for convenience as $I_{FG}\equiv I_F$ and $I_0/I_1\equiv R$. The Tl^{203} to Tl^{205} isotope shift is 1.8 kMc/sec and the Doppler width is in the range of 1.5 kMc/sec, but the overlap of one isotope radiation at the other isotope will still be reasonably constant over the 80 Mc/sec width of the $6\,^2D_{3/2}$ state levels and can be considered as merely contributing to the value of I_F. The angular dependence of a $\Delta m=2$ level-crossing signal is:

$$[(aa'+bb')^2-(a'b-ab')^2][\cos2(\varphi-\varphi')-\omega\sin2(\varphi-\varphi')]+[2(aa'+bb')(a'b-ab')]\times[-\sin2(\varphi-\varphi')+\omega\cos2(\varphi-\varphi')],\quad(26)$$

where

$$a=\cos\theta\cos\alpha,\quad b=\sin\alpha,\quad a'=\cos\theta'\cos\alpha',\quad b'=\sin\alpha',$$

$\omega=1/\hbar(E_{G,n}-E_{G',n\pm2})$, the θ, φ, θ', φ' angles are defined below Eq. (12), and $\cos\alpha=\hat{e}\cdot\hat{\theta}$ and $\cos\alpha'=\hat{e}'\cdot\hat{\theta}'$. Since the incident radiation is unpolarized, we evaluate Eq. (26) with $\alpha=0$ and with $\alpha=\pi/2$ and add the results. The remaining $\Delta m=2$ angular dependence is then:

$$\sin^2\theta((b'^2-a'^2)[\cos2(\varphi-\varphi')-\omega\sin2(\varphi-\varphi')]+2b'a'[-\sin2(\varphi-\varphi')+\omega\cos2(\varphi-\varphi')]).\quad(27)$$

The "Lorentzian"-shaped crossing signal comes from the terms without ω coefficients. It was selected in this experiment by using the scattering angles $\theta=\theta'=\varphi-\varphi'=\pi/2$, $\alpha'=\pi/2$. These angles can be used to obtain simple expressions for the $f_{m\mu}$ and $g_{m\mu}$ before performing the summations in Eq. (25), since all $\Delta m=2$ crossing terms would simply be multiplied by Eq. (27) if the angles were left arbitrary. The final result, from Eq. (25), is Eq. (28). The $G=G'$, $n=n'$ terms in Eq. (25) lead to the first three terms of Eq. (28). The $n'-n=0$, $G'-G=\pm1$ elements lead to the next three terms, and all the others are from the $n'=n=\pm2$ elements.

$$\begin{aligned}\bar{S}\propto{}&340+\frac{12x^4}{\delta_1^2\delta_{-1}^2}-4k\left[24-\frac{1-\frac{5}{2}x+x^2}{\delta_1^2}-\frac{1+\frac{5}{2}x+x^2}{\delta_1^2}\right]+\frac{6+3kx}{\delta_1^2}\frac{1}{1+4b^2\delta_1^2}+\frac{6-3kx}{\delta_{-1}^2}\frac{1}{1+4b^2\delta_{-1}^2}\\&+\left[12+\frac{6+12x^2}{\delta_1\delta_{-1}}-3k\left(1+\frac{1}{\delta_1}+\frac{1}{\delta_{-1}}+\frac{1+x^2}{\delta_1\delta_{-1}}\right)\right]\frac{1}{1+b^2(4x+\delta_{-1}-\delta_1)^2}+\left[12+\frac{6+12x^2}{\delta_1\delta_{-1}}-3k\left(1-\frac{1}{\delta_1}-\frac{1}{\delta_{-1}}+\frac{1+x^2}{\delta_1\delta_{-1}}\right)\right]\\&\times\frac{1}{1+b^2(4x-\delta_{-1}+\delta_1)^2}+\left[12-\frac{6+12x^2}{\delta_1\delta_{-1}}-3k\left(1-\frac{1}{\delta_1}+\frac{1}{\delta_{-1}}-\frac{1+x^2}{\delta_1\delta_{-1}}\right)\right]\frac{1}{1+b^2(4x+\delta_{-1}+\delta_1)^2}\\&+\left[12-\frac{6+12x^2}{\delta_1\delta_{-1}}-3k\left(1+\frac{1}{\delta_1}-\frac{1}{\delta_{-1}}-\frac{1+x^2}{\delta_1\delta_{-1}}\right)\right]\frac{1}{1+b^2(4x-\delta_{-1}-\delta_1)^2}+\frac{12(1+x/\delta_0)}{1+b^2(1+3x+\delta_0)^2}+\frac{12(1-x/\delta_0)}{1+b^2(1-3x+\delta_0)^2}\\&+\frac{12(1-x/\delta_0)}{1+b^2(1+3x-\delta_0)^2}+\frac{12(1+x/\delta_0)}{1+b^2(1-3x-\delta_0)^2},\end{aligned}\quad(28)$$

where

$$k\equiv(I_1-I_0)/I_1\equiv 1-R,\quad b\equiv 2\pi\tau a=a/\Gamma,\quad \delta_m\equiv(1-mx+x^2)^{1/2}.$$

APPENDIX III

To calculate the effect of $6s7s6d$ (or any $6sns6d$) and $6s6p^2$ configurational mixing on the $6\,^2D_{3/2}$ and $6\,^2D_{5/2}$ state hfs, we will expand these states as follows:

$$\psi(6\,^2D_{J,m})=\sum_{i=0}^{3} d_i\psi^i{}_{J,m}, \tag{29}$$

where

$$\begin{aligned}&\psi^0{}_{J,m}=(6s^26d)\,^2D_{J,m}, && \psi^2{}_{J,m}=(6s7s[^1S_0]6d)\,^2D_{J,m},\\ &\psi^1{}_{J,m}=(6s7s[^3S_1]6d)\,^2D_{J,m}, && \psi^3{}_{J,m}=(6s6p^2)\,^2D_{J,m},\end{aligned} \tag{30}$$

$$\sum_{i=0}^{3} d_i{}^2=1,\quad \text{and}\quad d_1,\ d_2,\ d_3\ll 1.$$

$\psi^1{}_{J,m}$ is a (core) $6s7s6d$ configuration in which the three outer electrons are coupled into a normalized $^2D_{J,m}$ state by Russell-Saunders coupling, with the $6s$ and $7s$ electrons first coupled into a $^3S_1$ state. Equivalent notation is used for the other $\psi^i{}_{J,m}$ states, and the d_i are the mixing coefficients (assumed identical) of the $6\,^2D_{3/2}$ and $6\,^2D_{5/2}$ states. As in Koster,[11] the dipole coupling constant is given by:

$$a(6\,^2D_J)=(-\mu/IJ)\langle\psi(6\,^2D_{J,m=J})\,|\sum_i H^i{}_z\,|\psi(6\,^2D_{J,m=J})\rangle, \tag{31}$$

where μ is the nuclear dipole moment, $\sum_i$ is the sum over the three outer electrons in each configuration, and $H^i{}_z$ is the hfs interaction of the ith electron, as defined by Koster. The required single-electron matrix elements of the hfs operator H_z are, in the nonrelativistic approximation:

$$\begin{aligned}&\langle\gamma,\ s=\tfrac{1}{2},\ l=0,\ m_s=\pm\tfrac{1}{2},\ m_l=0\,|H_Z|\,\gamma',\ \tfrac{1}{2},\ 0,\ \pm\tfrac{1}{2},\ 0\rangle=-(8\pi\mu_0/3)\,|\psi_\gamma(0)\psi_{\gamma'}(0)|,\\ &\langle\gamma,\ \tfrac{1}{2},\ l\neq 0,\ m_s,\ m_l|\,H_Z\,|\gamma',\ \tfrac{1}{2},\ l,\ m_s,\ m_l\rangle=-2\mu_0\langle r^{-3}\rangle_{\gamma\gamma'}\left[m_l-2m_s\frac{3m_l^2-l(l+1)}{(2l-1)(2l+3)}\right],\\ &\langle\gamma,\ \tfrac{1}{2},\ l\neq 0,\ \tfrac{1}{2},\ m_l|\,H_Z\,|\gamma',\ \tfrac{1}{2},\ l,\ -\tfrac{1}{2},\ m_l+1\rangle=3\mu_0\langle r^{-3}\rangle_{\gamma\gamma'}\frac{(2m_l+1)[(l+m_l+1)(l-m_l)]^{1/2}}{(2l-1)(2l+3)}.\end{aligned} \tag{32}$$

To use Eq. (32) in evaluating Eq. (31), we must express the $\psi^i{}_{J,m}$ in terms of the single-electron functions. Only the states with $m=J$ are required for our calculation, which are:

$$\begin{aligned}&\psi^0{}_{3/2,3/2}=\frac{1}{\sqrt{5}}[(0_1{}^+0_1{}^-1_3{}^+)-2(0_1{}^+0_1{}^-2_3{}^-)],\\ &\psi^1{}_{3/2,3/2}=\frac{1}{\sqrt{30}}[2(0_1{}^+0_4{}^+1_3{}^-)-(0_1{}^+0_4{}^-1_3{}^+)+(0_1{}^-0_4{}^+1_3{}^+)]-\frac{2}{\sqrt{30}}[(0_1{}^+0_4{}^-2_3{}^-)+(0_1{}^-0_4{}^+2_3{}^-)-2(0_1{}^-0_4{}^-2_3{}^+)],\\ &\psi^2{}_{3/2,3/2}=\frac{1}{\sqrt{10}}[(0_1{}^+0_4{}^-1_3{}^+)-(0_1{}^-0_4{}^+1_3{}^+)]-\frac{2}{\sqrt{10}}[(0_1{}^+0_4{}^-2_3{}^-)-(0_1{}^-0_4{}^+2_3{}^-)],\\ &\psi^3{}_{3/2,3/2}=\frac{1}{\sqrt{10}}[(0_1{}^+1_2{}^-0_2{}^+)+(0_1{}^+0_2{}^-1_2{}^+)-2\sqrt{2}(0_1{}^-1_2{}^-1_2{}^+)],\\ &\psi^0{}_{5/2,5/2}=(0_1{}^+0_1{}^-2_3{}^+),\\ &\psi^1{}_{5/2,5/2}=\frac{1}{\sqrt{6}}[2(0_1{}^+0_4{}^+2_3{}^-)-(0_1{}^+0_4{}^-2_3{}^+)-(0_1{}^-0_4{}^+2_3{}^+)],\\ &\psi^2{}_{5/2,5/2}=\frac{1}{\sqrt{2}}[(0_1{}^+0_4{}^-2_3{}^+)-(0_1{}^-0_4{}^+2_3{}^+)],\\ &\psi^3{}_{5/2,5/2}=(0_1{}^+1_2{}^+1_2{}^-).\end{aligned} \tag{33}$$

Each single-electron function has been written in the notation $m_i^{\pm}=|i, m_l=m, m_s=\pm\frac{1}{2}\rangle$ ($i=1, 2, 3, 4$ for $6s$, $6p$, $6d$, $7s$, respectively), and each three-electron configuration is represented by $(m_i^{\pm}m_j^{\pm}m_k^{\pm})\equiv|i,m_l,m_s\rangle|j,m_l,m_s\rangle \times|k,m_l,m_s\rangle$. Equation (31) can now be evaluated using Eqs. (30), (32), and (33) to give the nonrelativistic results:

$$a(6\,^2D_{3/2})=\frac{2\mu\mu_0}{3I}[(4.8-1.6d_1^2-4.8d_3^2)\langle r^{-3}\rangle_{6d,6d}-3.35d_1^2(\sigma^2+S^2)+5.8d_1d_2(S^2-\sigma^2)$$
$$-2.9d_0d_1S\sigma+3.6d_3^2\langle r^{-3}\rangle_{6p,6p}-5d_3^2S^2],$$
$$a(6\,^2D_{5/2})=\frac{2\mu\mu_0}{5I}[(3.43+0.8d_1^2-3.43d_3^2)\langle r^{-3}\rangle_{6d,6d}+5.6d_1^2(\sigma^2+S^2)-9.7d_1d_2(S^2-\sigma^2)$$
$$+4.35d_0d_1S\sigma+4d_3^2\langle r^{-3}\rangle_{6p,6p}+8.4d_3^2S^2], \tag{34}$$

where $S=|\psi_{6s}(0)|$, $\sigma=|\psi_{7s}(0)|$. With $d_0=1$, $d_1=d_2=d_3=0$, and the relation[35]

$$\langle r^{-3}\rangle_{\gamma\gamma}=\frac{\delta W_0}{2\mu_0^2(L+\frac{1}{2})Z_iH_r(L,Z_i)}$$

these equations reduce to Eq. (15) with $\epsilon=\delta=0$ and the relativistic correction $F_r(J,Z_i)$ neglected [$F_r(\frac{3}{2},71)=1.12$, $F_r(\frac{5}{2},71)=1.05$]. Relativistic corrections to the $\langle r^{-3}\rangle_{6p,6p}$ terms have also been neglected since the last term is a much larger d_3^2 contribution.

We may evaluate S, σ and the $\langle r^{-3}\rangle$ values as follows: Using a formula of Fermi and Segrè:[10]

$$\sigma^2=\frac{1}{a_0^3}\left(\frac{Z}{\pi n^{*3}}\right)\frac{dn^*}{dn}\left(\frac{1}{1-\beta^2Z^2}\right)^2=\frac{6.05}{a_0^3},\quad a_0=\text{Bohr radius}.$$

Assuming the $7\,^2S_{1/2}$ state hfs is due entirely to the $7s$ electron, and using Eq. (32) and the equivalent of Eq. (31) for the $7s$ state,

$$\sigma^2=3Ia(7\,^2S_{1/2})/16\pi\mu\mu_0=4.65/a_0^3.$$

From Kopferman's analysis of the Tl II spectrum,[35] $a(6s)=5.3$ cm^{-1}; so again from Eqs. (31) and (32)

$$S^2=3Ia(6s)/16\pi\mu\mu_0=60/a_0^3.$$

From the $6\,^2P_{1/2,3/2}$ fine structure δW_0,[35]

$$\langle r^{-3}\rangle_{6p,6p}=\frac{\delta W_0}{2\mu_0^2(L+\frac{1}{2})H_r(L,Z_i)Z_i}=\frac{9.5}{a_0^3}.$$

From the $6\,^2P_{1/2,3/2}$ hfs, and noting that the configuration interaction adds to $a(^2P_{3/2})$ what it subtracts from $a(^2P_{1/2})$ in the limit (assumed valid) of $\alpha_1^2\langle r^{-3}\rangle_{6p6p}/c\ll1$,[12]

$$a(^2P_{1/2})=(2\mu\mu_0/I)2.67F_{1/2}\langle r^{-3}\rangle_{6p,6p}+a_s,$$
$$a(^2P_{3/2})=(2\mu\mu_0/I)0.54F_{3/2}\langle r^{-3}\rangle_{6p,6p}-a_s. \tag{35}$$

So that

$$\langle r^{-3}\rangle_{6p,6p}=\frac{(a_{1/2}+a_{3/2})I}{2\mu\mu_0(2.67F_{1/2}+0.54F_{3/2})}=\frac{10.4}{a_0^3}$$

and

$$a_s=\frac{4.75}{a_0^3}\frac{2\mu\mu_0}{I}.$$

From the $6\,^2D_{3/2,5/2}$ fine structure,

$$\langle r^{-3}\rangle_{6d,6d}=\frac{\delta W_0}{2\mu_0^2(l+\frac{1}{2})H_r(2,Z_i)}=\frac{0.072}{a_0^3}.$$

Consequently, we will use the values $S=7.7a_0^{-3/2}$, $\sigma=2.2a_0^{-3/2}$, $\langle r^{-3}\rangle_{6p,6p}=10a_0^{-3}$, $\langle r^{-3}\rangle_{6d,6d}=0.072a_0^{-3}$ in Eq. (34) and arrive at:

$$a(6\,^2D_{3/2})=(2\mu\mu_0/3Ia_0^3)[0.35-215d_1^2$$
$$+310d_1d_2-50d_0d_1-260d_3^2],$$
$$a(6\,^2D_{5/2})=(2\mu\mu_0/5Ia_0^3)[0.25+360d_1^2$$
$$-520d_1d_2+74d_0d_1+530d_3^2]. \tag{36}$$